BILINGUAL PUBLISHING CO.
Pioneer of Global Academics Since 1984

Journal of Electronic & Information Systems

Volume 3 • Issue 1 • April 2021 ISSN 2661-3204 (Online)

Volume 3 Issue 1 • April 2021 • ISSN 2661-3204 (Online)

Journal of Electronic & Information Systems

BILINGUAL PUBLISHING CO.

Pioneer of Global Academics Since 1984

BILINGUAL PUBLISHING CO.
Pioneer of Global Academics Since 1984

Volume 3 | Issue 1 | April 2021 | Page1-39
Journal of Electronic & Information Systems

Contents

Articles

BILINGUAL PUBLISHING CO.
Pioneer of Global Academics Since 1984

Journal of Electronic & Information Systems
https://ojs.bilpublishing.com/index.php/jeis

ARTICLE

Non-fragile Dynamic Output Feedback H∞ Control for a Class of Uncertain Switched Systems with Time-varying Delay

Yuning Song Yuzhong Liu*

School of mathematics and Systems Science, Shenyang Normal University, Shenyang, Liaoning, 110034, China

ARTICLE INFO

Article history
Received: 7 May 2021
Accepted: 11 May 2021
Published Online: 13 May 2021

Keywords:
Single Lyapunov function
Uncertainty
H_∞ control
Non-fragile
Output feedback

ABSTRACT

The problem of non-fragile dynamic output feedback H_∞ control for a class of uncertain switched systems with time-varying delay is discussed. Firstly, the form of non-fragile dynamic output feedback H_∞ controller is given. Under the condition that the upper bound of time delay and the upper bound of delay derivative are limited simultaneously, Lyapunov functional and its corresponding switching rules are constructed by using single Lyapunov function method and convex combination technique; Secondly, we use the inequality lemma to scale the derived Lyapunov functional in order to eliminate the time-varying delay term in the inequality, and then introduce the J-function to obtain a nonlinear matrix inequality that satisfies the H_∞ performance index γ, we also employ Schur complement lemma to transform the nonlinear matrix inequality into set of linear matrix inequalities consisting of two linear matrix inequalities, a sufficient condition for the existence of a non-fragile dynamic output feedback H_∞ controller and satisfying the H_∞ performance index γ is concluded for a class of uncertain switching systems with variable time delay; Finally, a switched system composed of two subsystems is considered and the effectiveness and practicability of the theorem are illustrated by numerical simulation with LMI toolbox.

1. Introduction

The switched system is a hybrid dynamical system consisting of a series of continuous-time subsystems and a rule that controls the switching between them. Liberzon D [1] summarized the research status of switching systems in the literature. The switched system has received extensive attention in the field of control. In the actual control a physical process, the uncertainty and time delay of the systems is often encountered, it is also the cause of systems instability and poor performance. In recent years, the problem of H_∞ control for linear time-delay systems with uncertainties has attracted much attention. The research on uncertainty can be divided into two categories: norm bounded uncertainty and polymorphic uncertainty. For example, in 1992, Xie L [2] et al. studied the problem of robust H_∞ control for linear systems with norm-bounded time-varying uncertainties; In 2001, Goncalves E N [3] et al. studied the design of controllers for systems with polymorphic uncertainty. In terms of the design of the controller by the traditional robust control method only needs to find the gain of the controller to make the closed-loop system stable. However, when the controller is digitally executed, due to the limited word length of the memory and

**Corresponding Author:*
Yuzhong Liu,
School of mathematics and Systems Science, Shenyang Normal University, Shenyang, Liaoning, 110034, China;
Email: 876258614@qq.com

 DOI: https://doi.org/10.30564/jeisr.v3i1.3205

the aging of components and other factors, the controller is also very sensitive to small changes in its own when relying on different design algorithms, resulting in a closed-loop system performance degradation or even unstable. It leads to a new problem: to design a controller that can withstand a certain range of parameter changes, that is, a non-fragile controller.

In 1997, Keel [4] and others first put forward the concept of "non-fragile". The explanation of fragile was further elaborated in some later published literature [5]. In recent years, more and more scholars are interested in non-fragile research. In 1998, Dorato P [6] and others studied the design of non-fragile controllers based on robust control. In addition, in many practical problems, the state of the systems can not be measured directly. In view of the cost and reliability of control implementation, it is more practical to adopt non fragile output feedback. Yu L [7] and others studied the design of robust memory less H_∞ controllers for linear time-delay systems with time-varying and bounded norms uncertainties; In 1997, Han H C [8] and others studied the LMI method of output feedback H_∞ controller design for linear time-delay systems; In 1998, Kokame H [9] and others studied the robust H_∞ performance of linear time-delay differential systems with time-varying uncertainties; In 2006, Yang G H [10] and others studied the design of non-fragile output feedback H_∞ controller for linear systems; In 2009, Li L [11] and others studied the non-fragile dynamic output feedback control of linear time-varying delay systems; In 2010, Y Wang [12] and others studied the design of non-fragile output feedback H_∞ controllers for linear systems; In 2013, Fernando T L [13] and others studied the output feedback guaranteed cost control problem of uncertain linear discrete systems. However, there are few researches on the non-fragile dynamic output feedback H_∞ control of time-varying time-delay switched systems with uncertainties.

In this paper, the problem of dynamic output feedback H_∞ control for a class of uncertain time-varying delay systems is studied. Assuming that the uncertainty is norm bounded and parameter uncertainty which the parametric form of the uncertain coefficient matrix is given. The dynamic output feedback controller is designed, which is substituted into the original systems to obtain a new closed-loop system. The corresponding switching rules and Lyapunov functional are constructed. By using convex combination technique, inequality scaling lemma, and Schur complement lemma, the set of linear matrix inequality satisfying the given H_∞ performance index γ is obtained and the original system is asymptotically stable and satisfies the performance index γ. The sufficient conditions for H_∞ control are obtained, and the validity of the theorem is verified by numerical simulation.

2. Description of the Problem

Consider a class of switched systems with time delay and uncertainties.

$$\begin{aligned}\dot{x}(t) &= (A_{\sigma(t)} + \Delta A_{\sigma(t)}(t))x(t) \\ &+(A_{d\sigma(t)} + \Delta A_{d\sigma(t)}(t))x(t-d(t)) \\ &+B_{\sigma(t)}u(t) + B_{1\sigma(t)}\omega(t)\end{aligned}$$

$$z(t) = C_{1\sigma(t)}x(t) + D_{1\sigma(t)}\omega(t)$$

$$y = C_{2\sigma(t)}x(t) + D_{2\sigma(t)}\omega(t)$$

$$x(t) = 0 \ , t \in [-h, 0) \tag{1}$$

Where $x(t) \in R^n$, $u(t) \in R^r$, $z(t) \in R^m$, $y(t) \in R^g$ and $\omega(t) \in R^q$ are state vector, control input vector, control output vector, measurement output vector and external disturbance input vector. A_i, A_{di}, B_i, B_{1i}, C_{1i}, C_{2i}, D_{1i}, D_{2i} are constant matrices with proper dimensions; $d(t)$ is a time-varying delay and is a continuous function satisfying: $0<\mathrm{d(t)}<\tau$, $\dot{d}(t) \le d < 1$. τ, d are known constants. $\omega(t) \in R^m$ is the interference input of limited energy; $\sigma : [0, \infty) \to M = \{1, 2, \cdots, n\}$ represents the handover rule of this systems, where *n* represents the *n* switching subsystems of the switching system. $\Delta A_i(t)$ and $\Delta A_{di}(t)$ represent the time-varying uncertainty in the model and satisfy the following form of norm bounded conditions

$$\Delta A_i(t) = H_{1i}F_i(t)E_{1i} \tag{2}$$

$$\Delta A_{di}(t) = H_{2i}F_i(t)E_{2i} \tag{3}$$

Where H_{1i}, H_{2i}, E_{1i} and E_{2i} are constant matrices with appropriate dimensions, $F_i(t)$ are unknown ma-

DOI: https://doi.org/10.30564/jeisr.v3i1.3205

trices with Lebesgue measurable elements and satisfy the conditions

$$F_i^T(t)F_i(t) \le I \tag{4}$$

The problem studied in this paper is to design dynamic non-fragile output feedback H_∞ controller for uncertain time-varying delay systems (1), as follows:

$$\dot{x}_c(t) = (A_{ci} + \Delta A_{ci}(t))x_c(t) + (B_{ci} + \Delta B_{ci}(t))y(t)$$

$$u_i(t) = (C_{ci} + \Delta C_{ci}(t))x_c(t) \tag{5}$$

makes the systems (1) be asymptotically stable and meet the given performance index γ. The uncertain terms $\Delta A_{ci}(t)$, $\Delta B_{ci}(t)$ and $\Delta C_{ci}(t)$ of the controller (5) represent uncertain gain perturbation and meet the conditions:

$$\Delta A_{ci}(t)=H_{3i}F_i(t)E_{3i}$$

$$\Delta B_{ci}(t)=H_{4i}F_i(t)E_{4i}$$

$$\Delta C_{ci}(t)=H_{5i}F_i(t)E_{5i} \tag{6}$$

condition (4) and (6), where H_{3i}, H_{4i}, H_{5i}, E_{3i}, E_{4i} and E_{5i} are constant matrices with appropriate dimensions. And (5) where A_{ci}, B_{ci} and C_{ci} are undetermined constant matrices with appropriate dimensions.

The closed-loop system is obtained by combining formula (1) and formula (5)

$$\begin{bmatrix} \dot{x}(t) \\ \dot{x}_c(t) \end{bmatrix} = \begin{bmatrix} A_{\sigma(t)} + \Delta A_{\sigma(t)}(t) & B_{\sigma(t)}(C_{ci} + \Delta C_{ci}(t)) \\ (B_{ci} + \Delta B_{ci}(t))C_{2\sigma(t)} & A_{ci} + \Delta A_{ci}(t) \end{bmatrix} * \begin{bmatrix} x(t) \\ x_c(t) \end{bmatrix} + \begin{bmatrix} A_{d\sigma(t)} + \Delta A_{d\sigma(t)}(t) \\ 0 \end{bmatrix} * x(t - d(t)) + \begin{bmatrix} B_{1\sigma(t)} \\ (B_{ci} + \Delta B_{ci}(t))D_{2\sigma}(t) \end{bmatrix} * \omega(t) \tag{7}$$

Aiming at the systems in this case, the problem to be solved in this paper is to find a sufficient condition for the existence of a non-fragile output feedback controller that satisfies the given H_∞ performance index γ for the uncertain time-varying delay system (1).

3. Main Results

Definition 1 Considering any given constant γ, uncertain time-varying time-delay switched system (1) in the presence of non-fragile dynamic output feedback gain with the form of additive perturbation, the Existing form of non-fragile dynamic output feedback H_∞ controller can be obtained, and the system satisfies the given constant γ. By using the corresponding switching rules, the systems (1) can be stabilized if there is an output feedback H_∞ controller of the form (5) and corresponding switching rules $\sigma(t)$. For a given performance index, the response of the closed-loop systems satisfy the following two conditions:

1) When external disturbance $\omega(t) = 0$, construct corresponding switching rules $\sigma(t)$, so that the systems (1) are asymptotically stable.

2) When the initial state of system (1) at t=0 is 0, the following inequality holds for all non-zero values $(t) \in L\ [0,T]$, $0 \le T < \infty$, as follows:

$$\|z\|_2 \le \gamma \|\omega(t)\|_2$$

Lemma 1 [12] For any constant ε>0, vector X, Y, there are

$$2X^TY \le \varepsilon X^TX + \varepsilon^{-1}Y^TY .$$

Lemma 2[12] For any constant ε>0 and proper dimensions matrices H, E and $F(t)$ satisfy $F^T(t)F(t)\le I$, there are

$$HF(t)E + E^TF^T(t)H^T \le \varepsilon^{-1}HH^T + \varepsilon E^TE$$

Theorem 1 For systems (1), the dynamic output feedback control law given by equation (5), where the controller parameter matrices are as follows:

$$A_{ci} = r_{1i}P_c^{-1}$$

$$B_{ci} = r_{2i}P_c^{-1}C_{2i}^T$$

$$C_{ci} = r_{3i}B_i^TP \tag{8}$$

Given a constant $\gamma > 0$, there are the following linear matrix inequalities

 DOI: https://doi.org/10.30564/jeisr.v3i1.3205

$$\sum_{i=1}^{n}\lambda_i\begin{bmatrix}M_{1i} & M_{2i}\\ M_{2i}^T & M_{3i}\end{bmatrix}<0,\sum_{i=1}^{n}\lambda_i\begin{bmatrix}N_{1i} & N_{2i}\\ N_{2i}^T & N_{3i}\end{bmatrix}<0 \tag{9}$$

having solutions for $P>0, P_c>0, r_{1i}, r_{2i}, r_{3i}$, given $\varepsilon_{\alpha i}>0$, ((α=1 2 … 7 , $\lambda_i \geq 0 (i \in \bar{N})$ and satisfying $\sum_{i=1}^{n}\lambda_i=1$ of n real number, then the systems (1) are asymptotically stable under the action of controller (5) and satisfy the given H_∞ norm bound γ .Where

$$M_{1i}=A_i^TP+PA_i+C_{1i}^TC_{1i}+C_{2i}^TC_{2i}+\varepsilon_{1i}E_{1i}^TE_{1i}$$
$$+\varepsilon_{3i}E_{2i}^TE_{2i}+\varepsilon_{7i}C_{2i}^TE_{4i}^TE_{4i}C_{2i}+\varepsilon_{2i}I$$
$$M_{2i}=\left[C_{1i}^TD_{1i}+PB_{1i}PH_{1i}PH_{2i}PA_{di}PB_iH_{5i}PB_i\right]$$

$$M_{3i}=diag\begin{bmatrix}D_{1i}^TD_{1i}+D_{2i}^TD_{2i}+\varepsilon_{4i}D_{2i}^TE_{4i}^TE_{4i}D_{2i}\\ -\gamma^2I-\varepsilon_{1i}I-[(1-d)\varepsilon_{3i}]I\\ -[(1-d)\varepsilon_{2i}]I]-\varepsilon_{5i}I-r_{3i}^{-2}I\end{bmatrix}$$

$$N_{1i}=2r_{1i}I+2r_{2i}^2C_{2i}^TC_{2i}+\varepsilon_{6i}E_{3i}^TE_{3i}+\varepsilon_{5i}E_{5i}^TE_{5i}$$

$$N_{2i}=\left[P_cH_{3i}\quad P_cH_{4i}\quad P_cH_{4i}\quad PB_i\right]$$

$$N_{3i}=diag\left[-\varepsilon_{6i}I\quad -\varepsilon_{7i}I\quad -\varepsilon_{4i}I\quad -I\right]$$

The switching rules are as follows:

$$\sigma(t)=\arg\min\{\begin{bmatrix}x(t)\\ \omega_i(t)\end{bmatrix}^{\mathrm{T}}R_i'\begin{bmatrix}x(t)\\ \omega_i(t)\end{bmatrix}+x_c^T(t)S_i'x_c(t), i\in M\} \tag{10}$$

Where

$$R_i'=\begin{bmatrix}R_i+C_{1i}^TC_{1i} & C_{1i}^TD_{1i}+PB_{1i}\\ D_{1i}^TC_{1i}+B_{1i}^TP & D_{1i}^TD_{1i}-\gamma^2I+D_{2i}^TD_{2i}\\ & +\varepsilon_{4i}D_{2i}^TE_{4i}^TE_{4i}D_{2i}\end{bmatrix}$$

$$S_i'=S_i+r_{2i}^2C_{2i}^TC_{2i}+\varepsilon_{4i}^{-1}P_cH_{4i}H_{4i}^TP_c$$

$$R_i=A_i^TP+PA_i+\varepsilon_{1i}E_{1i}^TE_{1i}+\varepsilon_{2i}I$$
$$+\varepsilon_{3i}E_{2i}^TE_{2i}+C_{2i}^TC_{2i}+\varepsilon_{7i}C_{2i}^TE_{4i}^TE_{4i}C_{2i}$$
$$+P[\varepsilon_{1i}^{-1}H_{1i}H_{1i}^T+[(1-d)\varepsilon_{2i}]^{-1}A_{di}A_{di}^T$$
$$+[(1-d)\varepsilon_{3i}]^{-1}H_{2i}H_{2i}^T+r_{3i}^2B_iB_i^T$$
$$+\varepsilon_{5i}^{-1}B_iH_{5i}H_{5i}^TB_i]P$$

$$S_i=A_{ci}^TP_c+P_cA_{ci}+\varepsilon_{6i}E_{3i}^TE_{3i}+\varepsilon_{5i}E_{5i}^TE_{5i}$$
$$+r_{2i}^2C_{2i}^TC_{2i}+P_c(\varepsilon_{6i}^{-1}H_{3i}H_{3i}^T$$
$$+\varepsilon_{7i}^{-1}H_{4i}H_{4i}^T)P_c+PB_iB_i^TP$$

When the switched systems (1) have the non-fragile dynamic output feedback H_∞ controller, the uncertain switched systems with time-varying delay (1) are asymptotically stable and satisfy the given performance index γ .

Proof For systems (6), let

$$\{(t_k,i_k)\mid i\in M;k=0,1,2,\cdots,0=t_0\leq t_1\leq\cdots\}$$

be the switching sequence formed on $t\in[0,\infty)$ corresponding to the switching rule. Therefore, the Lyapunov function has the following form:

$$V(t)=V_1(t)+V_2(t)$$

$$V_1(t)=\begin{bmatrix}x(t)\\ x_c(t)\end{bmatrix}^T\begin{bmatrix}P & 0\\ 0 & P_c\end{bmatrix}\begin{bmatrix}x(t)\\ x_c(t)\end{bmatrix}$$

$$V_2(t)=\int_{t-d(t)}^{t}x^T(s)(\varepsilon_{2i}I+\varepsilon_{3i}E_{2i}^TE_{2i})x(s)ds$$

The time derivative along the systems (6) is obtained, as follows:

$$\dot V(t)=\dot x^T(t)Px(t)+x^T(t)P\dot x(t)$$
$$+\dot x_c^T(t)P_cx_c(t)+x_c^T(t)P_c\dot x_c(t)$$
$$+x^T(t)(\varepsilon_{2i}I+\varepsilon_{3i}E_{2i}^TE_{2i})x(t)$$
$$-(1-\dot d(t))x^T(t-d(t))(\varepsilon_{2i}I$$
$$+\varepsilon_{3i}E_{2i}^TE_{2i})x(t-d(t))$$

Firstly, the internal stability of the systems is considered, set $\omega(t)=0$, combine lemma 1, 2 and equations

DOI: https://doi.org/10.30564/jeisr.v3i1.3205

(2), (3), (4), (5), (6), there are

$$\dot{V}(t) \le x^T(t)R_i x(t) + x_c^T(t)S_i x_c(t) \tag{11}$$

According to equation (11), as long as $R_i < 0$, $S_i < 0$, there is $\dot{V}(t) < 0$. Then the systems (7) is asymptotically stable.

Secondly, when $\omega(t) \neq 0$, under zero initial conditions $x(t_0) = 0$, the J function is introduced,

$$J = \int_0^\infty (Z_i^T Z_i(t) - \gamma^2 \omega_i^T(t)\omega(t))dt \le$$

$$\int_0^\infty (Z_i^T Z_i(t) - \gamma^2 \omega_i^T(t)\omega(t) + \dot{V}(t))dt \le$$

$$\int_0^\infty \begin{bmatrix} x^T(t) & \omega_i^T(t) \end{bmatrix} R_i' \begin{bmatrix} x(t) \\ \omega_i(t) \end{bmatrix} dt + \int_0^\infty x_c^T(t) S_i' x_c(t) dt \ ,$$

where

$$R_i' = \begin{bmatrix} R_i + C_{1i}^T C_{1i} & C_{1i}^T D_{1i} + PB_{1i} \\ D_{1i}^T C_{1i} + B_{1i}^T P & D_{1i}^T D_{1i} - \gamma^2 I + D_{2i}^T D_{2i} \\ & +\varepsilon_{4i} D_{2i}^T E_{4i}^T E_{4i} D_{2i} \end{bmatrix}$$

$$S_i' = S_i + r_{2i}^2 C_{2i}^T C_{2i} + \varepsilon_{4i}^{-1} P_c H_{4i} H_{4i}^T P_c$$

When $R_i' < 0$, $S_i' < 0$, there are $J < 0$. The systems (1) satisfy the H_∞ performance index γ and are gradually stable under the action of the non-fragile dynamic output feedback controller (4). The Schur complement lemma is further used to make the $R_i' < 0$, $S_i' < 0$. It is equivalent to LMI of formula (8) in the theorem. And in the case of no disturbance input, $\dot{V}(t) < 0$ can still hold, then the theorem is proved.

4. Simulation Example

Given two uncertain time-varying delay continuous subsystems to form a linear switched systems (1).Where

$$A_1 = \begin{bmatrix} -5 & -2 \\ 0 & -6 \end{bmatrix},\ A_2 = \begin{bmatrix} -5.5 & 1 \\ -1 & -6 \end{bmatrix},$$

$$A_{d1} = \begin{bmatrix} 0 & 0.3 \\ 0.1 & 0.4 \end{bmatrix},\ A_{d2} = \begin{bmatrix} 0 & 0.3 \\ -0.2 & 0.5 \end{bmatrix},$$

$$B_1 = \begin{bmatrix} 1 \\ 0.5 \end{bmatrix}, B_2 = \begin{bmatrix} 0 \\ 1 \end{bmatrix}, B_{11} = \begin{bmatrix} 1 \\ 1.5 \end{bmatrix}, B_{12} = \begin{bmatrix} 1 \\ 1.5 \end{bmatrix},$$

$$C_{11} = C_{12} = \begin{bmatrix} 0.1 & 0 \\ 0 & 0.1 \end{bmatrix}, C_{21} = C_{22} = \begin{bmatrix} 1 & 3 \end{bmatrix},$$

$$D_{11} = D_{12} = \begin{bmatrix} 0 \\ 0 \end{bmatrix}, D_{21} = D_{22} = 1,$$

$$H_{11} = H_{12} = \begin{bmatrix} 0.2 \\ 0.1 \end{bmatrix}, E_{11} = E_{12} = \begin{bmatrix} 0.2 & 0 \end{bmatrix},$$

$$E_{21} = E_{22} = \begin{bmatrix} 0.5 & 0 \end{bmatrix},\ E_{41} = E_{42} = 0.1,$$

$$H_{51} = H_{52} = 0.1,$$

$$H_{21} = H_{22} = \begin{bmatrix} 0.3 \\ 0.15 \end{bmatrix},$$

$$H_{31} = H_{32} = H_{41} = H_{42} = \begin{bmatrix} 0.1 \\ 0.2 \end{bmatrix},$$

$$F_1(t) = F_2(t) = \sin(t).$$

The time delay is taken as 0.5, λ_1=0.4, λ_2=0.6, $d = 0.9$, $\varepsilon_{\alpha i}$=1,(α=1 2 ⋯ 7;i=1,2 .By solving linear matrix inequality (9) to get

$$P = \begin{bmatrix} 123.8791 & -83.3075 \\ -83.3075 & 57.8461 \end{bmatrix},$$

$$P_c = 1\times10^8 \begin{bmatrix} 1.8904 & -0.9448 \\ -0.9448 & 0.4728 \end{bmatrix}.$$

We substitute r_{11} = -2.8628×10^8, $r_{21} = 5.7130\times10^3$, $r_{31} = 7.2021\times10^{-5}$ into (8) to get

$$A_{c1} = 1\times10^3 \begin{bmatrix} -1.3283 & -2.6546 \\ -2.6546 & -5.3112 \end{bmatrix},$$

 DOI: https://doi.org/10.30564/jeisr.v3i1.3205

$$B_{c1}=\begin{bmatrix}0.1854\\0.3709\end{bmatrix}, C_{c1}=\begin{bmatrix}0.0059 & -0.0039\end{bmatrix};$$

We substitute $r_{12}=-4.2942\times10^{8}$, $r_{22}=4.7629\times10^{3}$, $r_{32}=7.2021\times10^{-5}$ into (8) to get

$$A_{c2}=1\times10^{3}\begin{bmatrix}-1.9924 & -3.9819\\-3.9819 & -7.9668\end{bmatrix},$$

$$B_{c2}=\begin{bmatrix}0.1546\\0.3093\end{bmatrix}, C_{c2}=\begin{bmatrix}-0.0060 & 0.0042\end{bmatrix}$$

The switching rules are as follows:

$$\sigma(x(t))=i=\begin{cases}1.if \begin{bmatrix}x(t)\\ \omega_i(t)\end{bmatrix}^{\mathrm{T}}(R_1'-R_2')\begin{bmatrix}x(t)\\ \omega_i(t)\end{bmatrix} \\ \quad +x_c^T(t)(S_1'-S_2')x_c(t)<0 \\ 2.if \begin{bmatrix}x(t)\\ \omega_i(t)\end{bmatrix}^{\mathrm{T}}(R_2'-R_1')\begin{bmatrix}x(t)\\ \omega_i(t)\end{bmatrix} \\ \quad +x_c^T(t)(S_2'-S_1')x_c(t)<0\end{cases}$$

5. Conclusions

In this paper, we study the problem of non-fragile dynamic output feedback H_∞ control for a class of switched systems with time-varying delay and norm-bounded uncertainty, a suitable switching rule is constructed by using a convex combination method and single Lyapunov function method. Furthermore, the derivative term of Lyapunov functional is scaled by using inequality lemma, and a sufficient condition for the problem to be solved is obtained in the form of matrix inequality which is only related to the upper bound of delay derivative. By using Schur complement lemma, the obtained matrix inequality is decomposed into a set of linear matrix inequalities. At the same time, we get the sufficient conditions of non-fragile H_∞ control for the uncertain switched systems with time-varying delay and present the specific form of the non-fragile dynamic output feedback H_∞ controller. The practicality and validity of the theorem are verified by numerical simulation examples. The results show that the non-fragile dynamic output feedback H_∞ controller theorem is valid for the systems, and the design method may be suitable for other types of systems.

Acknowledgment

This work is partially supported by science basic research program of the education department of Liaoning Province (No. LJC202002).The authors also gratefully acknowledge the helpful comments and suggestions of the reviewers, which have improved the presentation.

References

[1] Liberzon D, Morse A S. Benchmark problems in stability and design of switched systems [J]. IEEE Control Systems Magazine, 1999, 19(5): 59-70.

[2] Xie L, de Souza C E. Robust H∞ control for linear systems with norm-bounded time-varying uncertainty. IEEE Trans-actions on Automatic Control, 1992, 37(8): 1188-1191.

[3] Goncalves E N , Palhares R M , Takahashi R. H/sub 2//H/sub /spl infin// filter design for systems with polytope-bounded uncertainty [J]. IEEE Transactions on Signal Processing, 2006, 54(9): 3620-3626.

[4] Keel L H, Bhattacharyya S P. Robust, fragile, or optimal? [J]. Automatic Control IEEE Transactions on, 1997, 42(8): 1098-1105.

[5] Makila P M. Comments on 'robust, fragile, or optimal?' [J]. IEEE Transactions on Automatic Control, September 1998, 43 (9): 1265-1268.

[6] Dorato P. Non-fragile controller design: an overview [C]. Proceedings of the American Control Conference, Philadelphia, June 1998: 2829-2831.

[7] Yu L, Chu J, Su H. Robust memoryless H∞ controller design for linear time-delay systems with norm-bounded time-varying uncertainty [J]. Automatica, 1996, 32(12): 1759-1762.

[8] Han H C, Chung M J. An LMI approach to H∞ controller design for linear time-delay systems [J]. Automatica, 1997, 33(4): 737-739.

[9] Kokame, H, Kobayashi, Mori T. Robust H. performances for linear delay-differential systems with time-varying uncertainties [J]. IEEE Transactions on Automatic Control, 1998, 43(2):223-226.

[10] Yang G H, Wang J L. Non-fragile H∞ output feedback controller design for linear systems [J]. Journal of Dynamic Systems Measurement & Control, 2003, 125(1): 117-123.

[11] Li L, Jia Y. Non-fragile dynamic output feedback control for linear systems with time-varying delay [J]. IET Control Theory and Applications, 2009, 3(8): 995-1005.

[12] Y Wang, H Zhang, D Yang, M Dong. H∞ output feedback control for uncertain systems with time-varying delays [C]. Chinese Control and Decision Conference, 2010: 1570-1575.

[13] Fernando T L, Phat V N, Trinh K. Output feedback guaranteed cost control of uncertain linear discrete systems with interval time-varying delays [J]. Applied Mathematical Modelling, 2013, 37(3): 1580-1589.

DOI: https://doi.org/10.30564/jeisr.v3i1.3205

BILINGUAL PUBLISHING CO.
Pioneer of Global Academics Since 1984

Journal of Electronic & Information Systems
https://ojs.bilpublishing.com/index.php/jeis

BRIEF REPORT

An Integrated Emergency Response Tool for Developing Countries: Case of Uganda

Swaib Kyanda Kaawaase* **Rodney Ekisa Simon**

Networks Department, College of Computing and Information Sciences, Makerere University, Kampala, Uganda

ARTICLE INFO

Article history
Received: 8 July 2021
Accepted: 12 July 2021
Published Online: 16 July 2021

Keywords:
Emergency-response
E-health
E-infrastructure
E-service
Health-care

ABSTRACT

This paper presents a First responder emergency response tool (EMApp) as a step towards achieving integrated emergency care in developing countries, the case of Uganda. The EMApp prototype has potential to support health emergency response from various emergency stakeholders. This innovation is in line with strategic plans to embrace technologies towards the establishment of integrated social services such as emergency healthcare services (EHS) in Uganda. We describe the prototype and provide its functionalities that can be further enhanced to enable access to emergency services and save life. The possible assumptions, potential challenges and recommendations to implement and deployment of such a system are provided. There is currently no such integrated emergency response system in Uganda as is the case in many other developing countries. For future studies, there is need to deploy the tool and assess its impact on the communities.

1. Introduction

Developing countries like Uganda face many challenges including poor (internet) infrastructure, unreliable power supply, and others which hinder the accessibility to (health, social or judicial) services. Public health systems in such developing countries are underfunded, understaffed, and struggling to deal with emergencies [1]. Non-theless mobile technologies have gained trust among communities and are being applied in various disciplines [2,3] including as health assistants and as financial transaction medium/platforms.

A good health system is one that responds well with emergencies, notably, the best health care systems globally [4,5] emphasize speed of access to health care and equitability of such access. Notably, no African health system is ranked among the first 50 best global health systems as of 2019 where South Africa ranks 53rd position [4]. Many Ugandans loose lives due to the ill state of health care access infrastructure especially in areas outside the cities and the remote.

The current growth in information communication technologies (ICT) and their wide uptake among the communities in developing countries offers a wide potential to enhance access to social services including emergency response services although less of such technologies have been utilized for access to emergency health care services (EHS) in the developing countries. On the other hand, in the developed world, customized apps and devices provide a range of services from health management to cost effective health care services at the patients' convenience [6]. Emergency care systems have the potential to avert half of all

**Corresponding Author:*
Swaib Kyanda Kaawaase,
Networks Department, College of Computing and Information Sciences, Makerere University, Kampala, Uganda;
Email: kswaibk@gmail.com

 https://doi.org/10.30564/jeisr.v3i1.3440

deaths in low- and middle-income countries (LMIC) [7].

Emergency health services comprise hospital emergency department, ambulance services and a number of aero-medical retrieval and transfer services that provide integrated medical care to people in acute illness and injury [6]. Such a service enables early recognition and lifesaving interventions for time sensitive situations in which delay in action may result in death, disability or render treatment less effective [8]. EHS range from on-scene care to a global demand to improve efficiency of health systems. In this work we consider emergency condition to include road traffic, trauma, infections, non-communicable diseases and complications of pregnancy which accounted for 90% of the leading death in low and middle income countries in 2017 [7]. The emergency panic/deficit brought by the COVID-19 outbreak has shown the ill preparedness of health systems and highlighted the need to priorities emergency services in Uganda [9].

We introduce 1st Responder's Emergency Mobile Application (EMApp) to address the delay in response time by first responders to emergencies due to inadequate, inaccurate and untimely communication between the incident reporter and first responders. EMApp will trace and track emergency information to such emergencies and providing emergency remedial information to those in emergencies that could lower the threat levels of a situation as they await rescue from first responders. EMApp is to be deployed in Kampala district where communication infrastructure is sufficient and inhabitants utilize the smart phones but also the area that is more prone to emergencies due to population density.

The pilot EMApp coverage includes

i. Ambulance service
ii. Police
iii. Fire Brigade

The rest of this paper is organized as follows; section 2 is on EMApp functionalities, section 3 describes the deployment requirements, while section 4 presents snapshots and describes usage, section 5 is a discussion and conclusion.

2. Materials and Methods

A survey on Uganda's health system was carried out in selected districts particularly to identify the hindrances. Major to the challenges was access to emergency health care, which is in line with literature [10-12]. An integrated emergency response prototype was developed while considering user requirements from the same survey. The tool is in such a way that emergency services are integrated so that the appropriate service is called up and the right stakeholder is contacted in time of emergency to save the victim.

2.1 Deployment and Target Users

The application is supported on android operating system 5 or higher and the iOS. The application inter-operates with GPS and google map systems. The application was developed using a distributed architecture wherein databases are distributed to different regions of the country to enable quick access and processing information requests. The application enables connectivity of different and independent emergency service providers to aggregate services and provide comprehensive emergency care.

2.1.1 Target Users

Emergency responders such as public health field workers who offer field service, the health authorities who receive timely reports from the system as well as the individuals who report the incidents. First responder is an insurance application to many sorts of incidents and therefore connects the emergency victim with the first responders to reduce risk on health. Law enforcement authorities can also utilize the tool in the case of forensic tracking. Researchers and developers of health instruments are potential users of the tool for further enhancement or development of related tools. Generally, EMApp can be used by all service providers whose line of work is emergency response. Users who need to dispatch or book resources at particular health institutions and quick relay of information to firefighting services are targeted.

2.1.2 Installation

The tool is installable on a dedicated server at the central health authority for better governance. The tool has a mobile application that is downloadable from google plays stores to be installed to mobile gadgets and used to register use for emergency services. The tool requires a national ID or passport for best validation at time of registration. The back end (dashboard) of the tool is an executable file that is installable on computer for administration of responses ie, monitoring, dispatch, reporting and tracking resources as well as ring-fencing resources required for a particular emergency.

2.1.3 Interfaces

For hardware interface: The First Responder's Emergency Mobile Application is an iOS and Android mobile application that is built using React Native programming language and will communicate with a PHP web admin controller.

Software interfaces; EMApp is an iOS and Android

https://doi.org/10.30564/jeisr.v3i1.3440

mobile application that is built using the PHP programming language. The primary data input into the system is in form of text and videos using the mobile application interface.

For communication interface; The application is a dependent mobile application that requires internet connectivity with need for a centralized server that will keep track of the emergency requests made and other data. The function enables liaison with other existing databases such as the national database (NDB), Police, insurance and hospital databases for optimized resource mobilization to suit the emergency at hand.

2.1.4 Documentation

The internal processes of the application have been documented with comments in all scripts. Specification document highlights all the user requirements interpreted as system functions. The users are provided a user manual for easy system usage. The user manual is aligned to the system requirements and hence functions for the optimal use of first responder tool.

Other documentation are suitable icon names that appropriately describe the function or response that is expected from the icons.

2.1.5 Assumptions for Suitable Deployment

The most important assumption is the availability of enabling infrastructure such as data communication network to enable communication and automated mobilization of resources to save life in a given emergency state. Other assumptions include availability of reliable response policing system and hospital response teams/system at registered hospitals. Also assumed is a willing and quick insurance response systems for the case of victims insured and response systems from other institutions required to save life in the emergency.

2.1.6 EMApp Functionalities

EMApp functions include user authentications and validation that is intended to reduce response to false and/or junk alarms by identifying the initiator of the emergency state in the system. The function is multifactor authentication based on user's prioritized authentication for example, the phone number used is legally registered to the person with a National ID (NID) or passport and such information can be probed from the NDB once the phone number is provided. The NID can easily be probed further for identify of the registered next of kin to the victim and notified of emergency. Biometrics (fingerprint and picture) is also registered in the NDB and hence ease of authentication verification and identification in case of catastrophic emergency rendering the victim unconscious. All this is possible through the inbuilt registration function that collects user details into the local database. The function of crime reporting involves the responder utilizing the app to send a crime report to the central policing authorities in various forms including compressed video or images while identifying and copying the closest police station to the crime scene. This function utilizes GPS and google maps to reduce to time of searching for the emergency service unit for example, nearest police station to take responsibility. The user (victim/requester) location function is also included for best estimate of distance to the nearest emergency services provider. Request emergency assistance function clearly identifies the type of emergency and prioritizes based on severely of the emergency. The function alerts the stakeholders to the emergency, these can include next of kin as registered on the NID, ambulance, insurance, legal personnel, domestic violence unit of police etc. The notify function implements SMS infrastructure to alert the next of kin but also email and web interface are inbuilt to report details of the emergency such as location coordinates (and nearby significant features), ID of the victim, brief crime report in order to elicit the right response to such an emergency.

The feedback function is necessary to generate important usability reports from the users in order to better the provided emergency services.

Donate function: although the service rendered by the EMApp is free, this function enables funds raising from voluntary beneficiaries or well-wishers for maintenance and continued service support.

3. Results

The results are presented as screenshots of the prototype below.

Figure 1. Startup Screen Interface

The user in emergency condition starts the application on their phone shown in Figure 1 and selects the specific

emergency category as in Figure 2 and initiates the emergency response by a single click to enable the application mobilize the right resources to save or assist the victim (s).

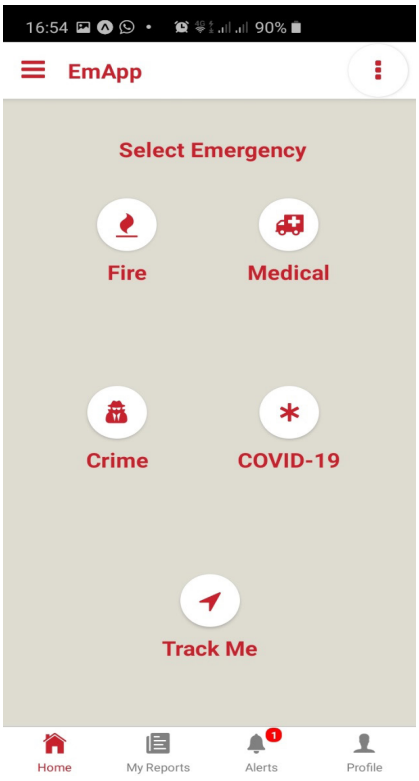

Figure 2. Home Interface or screen for selection of emergency category

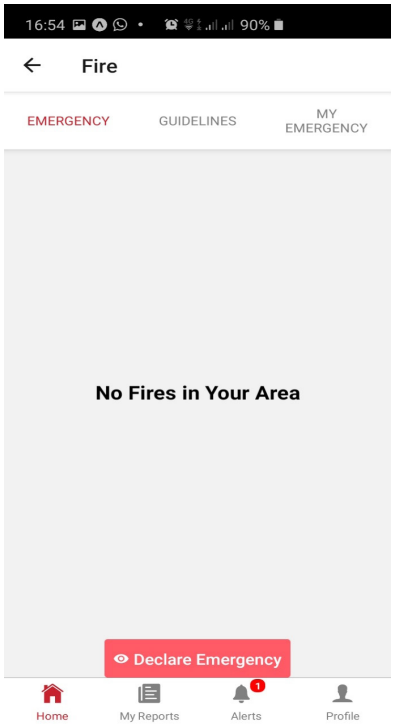

Figure 3. Selected Fire emergency

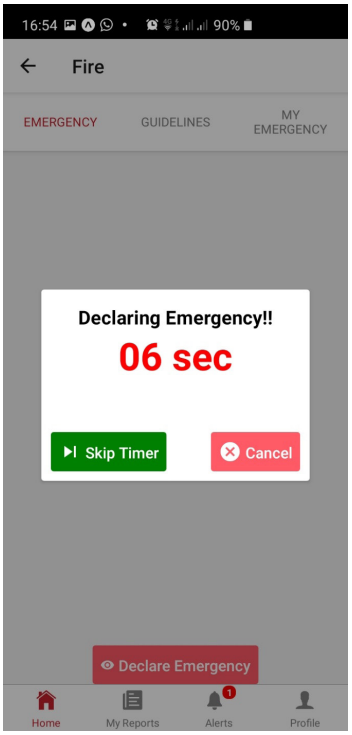

Figure 4. Declaration of Fire Emergency

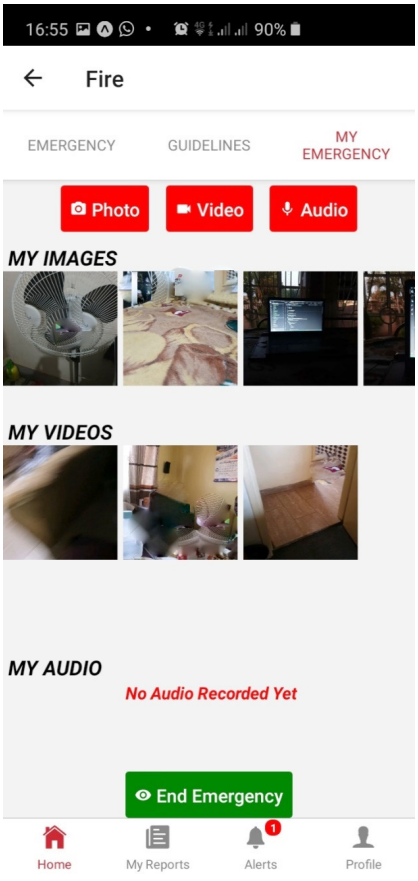

Figure 5. Interface to allow recording media in an emergency

https://doi.org/10.30564/jeisr.v3i1.3440

The user opts for suitable media in which they want to log the emergency.

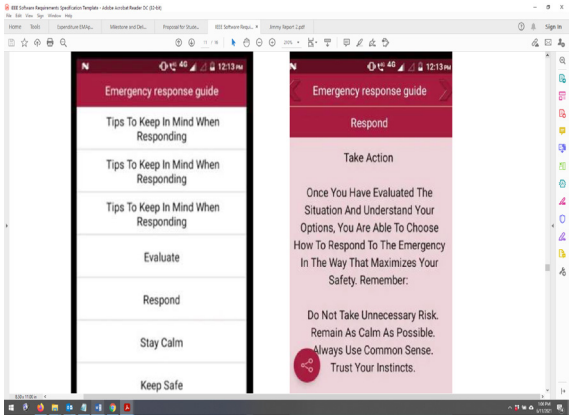

Figure 6. Emergency Response Guidelines and details screenshots

4. Discussion

The presented prototype is work in progress towards an integrated emergency first responder system that has potential to save many lives when deployed in Uganda or other countries where no emergency response system exists. The tool is evidently convenient to be utilized when faced with an emergency as evidenced in the screenshots.

EMApp is a step towards deployment of an integrated emergency response system for developing countries like Uganda and hence the focus should be on the additional scope towards reaching the integrated emergency services. It is imperative to establish a cost–effectiveness database to support the development and implementation of a scaled emergency response system for developing countries. Such database should form basis to inform policy makers and regulators on and assist prioritization for health and economic benefit.

The tool is recommended to complement the command and control functions [10] of major emergency management operations such as in hospitals, health providing insurance, private ambulance services for better functioning and coordination of the emergency services. For future studies, there is need to deploy the tool and assess its impact on the health sector in Uganda. There is also need for inclusiveness by providing speech recognition and other functionalities for persons with disabilities (PWD), the tool should be compatible with hearing aid.

For better accessibility, emergency service should be accessible through a USSD code and verifying with already provided records such as national ID or passport before dispatch of service. This enables access by non-smartphone holders but possess the basic phone and these are a large percentage of the phone users.

5. Conclusions

An integrated emergency response tool was developed and presented in this report. Uptake of the tool among the developing nations could enhance access to emergency care and save lives in time of emergency.

Author Contributions

Swaib Kyanda Kaawaase is the supervisor and part of the development team, a critical advisor and writer of this manuscript documenting the work done on the project.

Ekisa Rodney is the key developer, a guide to the direction of the project. He is also contributor to sections of the manuscript and reviewer.

Conflict of Interest

No conflict of interest to declare.

Funding:

This project received two (2) college local seed grants (2018 and 2019) from Research, Innovations, Services and Engagement (RISE) of the College of Computing and Information Sciences at Makerere University.

Acknowledgments

We acknowledge the various emergency stakeholders that we visited during the survey to understand the problem at hand. We also acknowledge Kasky Technologies for the secretariat provided in preparing this manuscript.

References

[1] Margaret E.Kruk, 2008, Emergency Preparedness and Public Health Systems: Lessons for Developing Countries, American Journal of Preventive Medicine, Pp 529-534, https://doi.org/10.1016/j.amepre.2008.02.012.

[2] Wikipedia, the online encyclopedia https://en.wikipedia.org/wiki/Mobile_technology_in_Africa, 23rd June 2021.

[3] Enock Yonazi, Tim Kelly, Naomi Halewood and Colin Blackman, 2012 "The Transformational Use of Information and Communication Technologies in Africa" eTransform AFRICA.
DOI: 10.1596/26791Corpus ID: 168833751.

[4] Sophie Ireland, 2019, "Revealed: Countries with the Best Health Care Systems, 2019" available on https://ceoworld.biz/2019/08/05/revealed-countries-with-the-best-health-care-systems-2019.

[5] BBC, https://www.bbc.com/news/health-40608253.

[6] Toloo Ghasem, Fitzgerald Gerard, Aitken Peter, Chu Kevin, Ting Joseph, Tippett, Vivienne, 2011, Emergency Health Services: Demand & Service Delivery Models- Monograph 1: Literature Review and Activity Trends. Queensland University of Technology.

ISBN: 978-1-921897-11-5.

[7] V.C. Kannan, A. Tenner, H.R. Sawe, M. Osiro, T. Kyobe, E. Nahayo, N.G. Rasamimanana, S. Kivlehan, and R. Moresky, 2020,"Emergency care systems in Africa: A focus on quality" Afr J Emerg Med. 2020; 10(Suppl 1): S65–S72.
DOI: 10.1016/j.afjem.2020.04.010.

[8] Kalin Werner, Nicholas Risko, Taylor Burkholder, Kenneth Munge, Lee Wallis & Teri Reynolds, Cost–effectiveness of emergency care interventions in low and middle-income countries: a systematic review, Bulletin of the World Health Organization 2020;98:341-352.
DOI: http://dx.doi.org/10.2471/BLT.19.241158.

[9] Patience Akumu, 2020 "A Review of COVID-19 and the Health Equality Dilemma in Uganda" Konrad Adenauer Stiftung - KAS.

[10] Brian S. Sorensen, Richard D. Zane, Barry E. Wante, Mitesh B. Rao, Michelangelo Bortolin, Gerald Rockenschaub 2011, Hospital emergency response checklist "An all-hazards tool for hospital administrators and emergency managers" World Health Organization.
DOI:10.13140/2.1.3047.6160.

[11] Dowhaniuk, N. Exploring country-wide equitable government health care facility access in Uganda. Int J Equity Health 20, 38 (2021). https://doi.org/10.1186/s12939-020-01371-5.

[12] Werner, K., Tracy Kuo Lin, Nicholas Risko, Martha Osiro, Joseph Kalanzi & Lee Wallis . The costs of delivering emergency care at regional referral hospitals in Uganda: a micro-costing study. BMC Health Serv Res 21, 232 (2021). https://doi.org/10.1186/s12913-021-06197-7.

https://doi.org/10.30564/jeisr.v3i1.3440

BILINGUAL PUBLISHING CO.
Pioneer of Global Academics Since 1984

Journal of Electronic & Information Systems
https://ojs.bilpublishing.com/index.php/jeis

ARTICLE

Study the Multiplication M-sequences and Its Reciprocal Sequences

Ahmad Al Cheikha[1*] Ebtisam Haj Omar[2]

1. Math. Sci.Dep., Ahlia Uni., Bahrain
2. Elect. Energy Dep., Tishreen Univ, Syria

ARTICLE INFO

Article history
Received: 2 August 2021
Accepted: 15 August 2021
Published Online: 30 August 2021

Keywords:
Binary sequences
Finite fields
Shift register
Equivalent binary linear shift register
Degree of complexity

ABSTRACT

M-Sequences play a big important role, as the other binary orthogonal sequences, for collection the information on the input links and distribution these information on the output links of the communication channels and for building new systems with more complexity, larger period, and security, through multiplication these sequences. In our article we try to study the construction of the multiplication sequence $\{z_n\}$ and its linear equivalent, this multiplication sequence is as multiple two sequences, the first sequence $\{a_n\}$ is an arbitrary M-sequence and the second sequence $\{b_n\}$ is not completely different but is the reciprocal sequence of the first sequence $\{a_n\}$ that is the reciprocal sequence has characteristic polynomial $g(x)$ is reciprocal of $f(x)$, which is the characteristic polynomial of the first sequence $\{a_n\}$, also we will study the linear equivalent of the multiplication sequence $\{z_n\}$ and we will see that the length of the linear equivalent of $\{z_n\}$ is equal to $((deg\, f(x))^2 - deg(f(x))$.

1. Introduction

Sloane, N.J.A., study the product or multiplication sequence $\{z_n\}$ on t degrees of $\{a_n\}$ which has the degree of complexity r and gave the answer that the degree of complexity of $\{z_n\}$ can't be exceeded ${}_rN_t = \binom{r}{1} + \binom{r}{2} + \ldots + \binom{r}{t}$.

M-Sequences are used in the forward links for mixing the information on connection and as in the backward links of these channels to receivers get the information in a correct form, especially in the pilot channels and in the sync channels [1-8].

Al Cheikha A. H., studied the construction of the multiplication binary M-Sequences and their complexities, periods, and the lengths of the linear equivalents of these multiplication sequences, where the multiplication will be on one M-Sequence or on more than one sequence and gave an Illustration of the answer of the question "why the linear shift register don't be reached the maximum length ${}_rN_t$", where the product or multiplication will be on h degrees of one M-Sequence, also, the length of the equivalent shift register of the multiplication sequence is equal to the product r by s, where, r and s are the length of the shift registers of the first and second sequences respectively and they are prime numbers [9-14].

2. Research Method and Materials

2.1 M- Sequences

The sequence $\{s_n\}$ of the form:

$$s_{n+k} = \gamma_{k-1}s_{n+k-1} + \gamma_{k-2}s_{n+k-2} + \ldots + \gamma_0 s_n + \gamma;\ \gamma\ \&\ \gamma_i \in F_2,\ i = 0,1,\ldots,k-1$$
$$or \qquad s_{n+k} = \sum_{i=0}^{k-1} \gamma_i s_{n+i} + \gamma \qquad (1)$$

**Corresponding Author:*
Ahmad Al Cheikha,
Math. Sci.Dep., Ahlia Uni., Bahrain;
Email: alcheikhaa@yahoo.com

 DOI: https://doi.org/10.30564/jeisr.v3i1.3507

Where, $\gamma, \gamma_0, \gamma_1, ..., \gamma_{k-1}$ are in the field F_2 and k is positive integer is called a binary linear recurring sequence of complexity or order k, *if* $\gamma = 0$ then the sequence is called homogeneous sequence (H.L.R.S), in other case the sequence is called non-homogeneous, the vector $(s_0, s_1, ..., s_{k-1})$ is called the initial vector and the characteristic equation of the sequence is:

$$f(x) = x^k + \gamma_{k-1}x^{k-1} + ... + \gamma_1 x + \gamma_0 \quad (2)$$

We are limited in our article to $\gamma_0 = 1$.

2.2 Definitions and Theorems

Definition 1

The binary sequence $\{s_n\}$ satisfies the following condition;

$$s_{n+r} = s_n \ ; \quad n = 0, 1, ...$$

Is called a periodic sequence and the smallest natural number r which not equal to zero is called the period of the sequence [2,6].

Definition 2

The L.F.S.R is a linear feedback shift register which contains only addition circuits and the general term of the sequence $\{s_n\}$ generated through the shift register is the term of the output of the register [3].

Definition 3

The vector $\overline{X} = (\overline{s_1}, \overline{s_2}, ..., \overline{s_n})$ is the complement of the vector $X = (s_1, s_2, ..., s_n), s_i \in F_2$ where

$$\overline{s_i} == 0 \ if \ s_i = 1 \ and \ \overline{s_i} = 1 \ if \ s_i = 0 \quad (3)$$ [2,6,7]

Definition 4

The coefficient of correlations function of two binary vectors $t = (t_0, t_1, ..., t_{n-1})$ and $l = (l_0, l_1, ..., l_{n-1})$ is

$$R_{t,l} = \sum_{i=0}^{n-1} (-1)^{t_i + l_i} \quad (4)$$

Where $t_i + l_i$ is computed by *mod* 2.

If $x_i, y_i \in \{1, -1\}$ (usually, replacing in binary vectors t and l each "1" by "1* = -1" and each "0" by "0*=1" then

$$R_{t,l} = \sum_{i=0}^{n-1} t_i^* l_i^* \quad (5)$$ [2-9]

Definition 5

If $|R_{t,l}| \le 1$ of the two vectors t and l then we said the vectors t and l are orthogonal [8-10].

Definition 6

If A is a set of binary vectors as the following:

$$A = \{t; t = (t_0, t_1, ..., t_{n-1}) \ x_i \in F_2, i = 0,1,..., n-1\}$$

The set A is orthogonal if and only if satisfies the following two conditions:

$$1. \ \forall t \in A, \left| \sum_{i=0}^{n-1} t_i^* \right| \le 1, \ or \ |R_{t,0}| \le 1. \quad (6)$$

$$2. \ \forall t, l \in A, \& \ t \ne l, \left| \sum_{i=0}^{n-1} t_i^* l_i^* \right| \le 1 \ \boldsymbol{o} \ |R_{t,l}| \le 1. \quad (7)$$ [6,9]

Definition 7

The maximum length of an equivalent binary liner feedback shift register is always less than or equal to the maximum length ${}_r N_t$ [2,3,8].

Definition 8

The reciprocal function of the function $f(x)$ is the function:

$$g(x) = x^n f(1/x) \quad (8)$$

Where, n is the degree of $f(x)$ [7].

Theorem 9

If $\{s_n\}$ is a H.L.R.S binary sequence with the complexity k, period r and its characteristic polynomial is $f(x)$ then $r \,|\, ord\, f(x)$ and if the polynomial $f(x)$ is primitive then the period of the sequence $\{s_n\}$ is $, 2^k - 1$ and this sequence is called M-Sequence [6, 12-15].

Lemma 10 (Fermat's theorem)

Each element x of the finite field F satisfies the equation:

$$x^q = x \quad (9)$$

Where q is the number of all elements in F [6,10].

Theorem 11

If $\{s_n\}$ is a homogeneous binary linear recurring sequence and $g(x)$ is its characteristic prime polynomial of degree k and λ is a root of $g(x)$ in any splitting field of F_2 then the general term of the sequence $\{s_n\}$ is:

$$s_n = \sum_{i=1}^{k} C_i \left(\lambda^{2^{i-1}} \right)^n \quad (11)$$ [6,12]

Theorem 12

$$\boldsymbol{i}. \ (q^m - 1) \,|\, (q^n - 1) \Leftrightarrow m \,|\, n \quad (12)$$

DOI: https://doi.org/10.30564/jeisr.v3i1.3507

ii. any subfield of the field F_{2^n} is a field of order 2^m where $m \mid n$ and if F_q is a field of order $q = 2^n$ then any subfield of it is has the order 2^m and $m \mid n$, and by inverse if $m \mid n$ then the field F_{2^n} contains a subfield of order 2^m [6,11-15].

*Our study is limited to the M-Sequence of the period $r = 2^k - 1$.

3. Results and Discussion

3.1 Multiplication Two Reciprocal Binary M-Sequences

If $\{a_n\}$ is a recurring M-Sequence of degree k and $f(x)$ is its characteristic prime polynomial (of degree k), which has the independent different roots $\alpha_1, \alpha_2, \ldots$, then general term of sequence $\{a_n\}$ will be given through the relation:

$$a_n = A_1\alpha_1^n + A_2\alpha_2^n + \ldots + A_k\alpha_k^n = \sum_{i=1}^{k} A_i\alpha_i^n \tag{13}$$

If the sequence $\{a_n\}$ in F_2, its characteristic prime polynomial is $f(x)$, and α is a root of $f(x)$ then the general term of the sequence $\{a_n\}$ is

$$a_n = A_1\alpha^n + A_2(\alpha^{2^{2-1}})^n + \ldots + A_k(\alpha^{2^{k-1}})^n = \sum_{i=1}^{k} A_i(\alpha^{2^{i-1}})^n \tag{14}$$

Suppose the recurring M-Sequence $\{b_n\}$ which has the characteristic prime polynomial $g(x)$, and $g(x)$ is the reciprocal of $f(x)$ and $\beta_1, \beta_2, \ldots, \beta_k$ are the different linear independent roots of $g(x)$, which are reciprocal of $\alpha_1, \alpha_2, \ldots, \alpha_k$, then $\{bn\}$ is

$$b_n = B_1\beta_1^n + B_2\beta_2^n + \ldots + B_k\beta_k^n = \sum_{i=1}^{k} B_i\beta_i^n$$

The sequence $\{b_n\}$ is called the reciprocal sequence of the sequence $\{a_n\}$.

Thus, if α_i is of the form $\alpha^{2^{i-1}}$ and β_i is reciprocal α_i then $\beta_i = \alpha^{2^k - 2^{i-1} - 1}$ and b_n will be written in the form

$$b_n = B_1\alpha^{n(2^k-2)} + B_2\alpha^{n(2^k-3)} + \ldots + B_k\alpha^{n(2^k-2^{k-1}-1)} = \sum_{i=1}^{k} B_i\alpha^{n(2^k-2^{i-1}-1)} \tag{15}$$

Thus

$$a_n b_n = \left(\sum_{i=1}^{k} A_i(\alpha^{2^{i-1}})^n\right)\left(\sum_{j=1}^{k} B_j(\alpha^{n(2^k-2^{j-1}-1)})^n\right) = \left(\sum_{i,j=1, i\neq j}^{k} A_iB_j(\alpha^{2^{i-1}})^n(\alpha^{n(2^k-2^{j-1}-1)})^n\right) + \left(\sum_{i=1}^{k} A_iB_i\right) \tag{16}$$

Example 1

Suppose the binary recurring sequence $\{a_n\}$ where

$a_{n+3} + a_{n+1} + a_n = 0$, or $a_{n+3} = a_{n+1} + a_n$ (17)

The characteristic equation of sequence is $x^3 + x + 1 = 0$ and its characteristic polynomial $f(x) = x^3 + x + 1$, if a is a root of the characteristic equation then α generates the field

$$F_{2^3} = \{0, \alpha^7 = 1, \alpha, \alpha^2, \alpha^3 = \alpha + 1, \alpha^4 = \alpha^2 + \alpha, \alpha^5 = \alpha^2 + \alpha + 1, \alpha^6 = \alpha^2 + 1\} \tag{18}$$

and a_n is given by the formula

$$a_n = A_1\alpha^n + A_2(\alpha^2)^n + A_3(\alpha^4)^n$$

For the initial vector ($a_0 = 0$, $a_1 = 1$, $a_2 = 0$) we have

$$\begin{cases} A_1 + A_2 + A_3 = 0 \\ \alpha A_1 + \alpha^2 A_2 + \alpha^4 A_3 = 1 \\ \alpha^2 A_1 + \alpha^4 A_2 + \alpha A_3 = 0 \end{cases}$$

Solution this gives us that $A_1 = \alpha^2, A_2 = \alpha^4, A_3 = \alpha$ and a_n is

$$a_n = \alpha^2(\alpha)^n + \alpha^4(\alpha^2)^n + \alpha(\alpha^4)^n \tag{19}$$

The periodic of $\{a_n\}$ is $2^3 - 1 = 7$ and we have the flowing sequence

0 1 0 1 1 1 0, 0 1 0 1 …….

The following Figure1, shows the shift register generating $\{a_n\}$

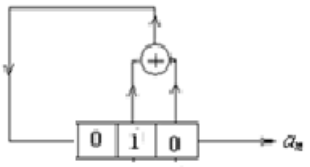

Figure 1. Shift register generating $\{a_n\}$

Suppose the binary recurring sequence $b_{n+3} + b_{n+2} + b_n = 0$ or $b_{n+3} = b_{n+2} + b_n$, its characteristic polynomial $g(x) = x^3 + x^2 + 1$ is prime and reciprocal of $f(x)$, the roots of $g(x)$ are

$$\beta_1 = \frac{\alpha^7}{\alpha} = \alpha^6, \beta_2 = \frac{\alpha^7}{\alpha^2} = \alpha^5, \beta_3 = \frac{\alpha^7}{\alpha^4} = \alpha^3 \tag{20}$$

Is very easy looking that $\alpha^6, \alpha^5, \alpha^3$ are roots of the characteristic polynomial $g(x)$ corresponding the roots $\alpha, \alpha^2, \alpha^4$ of $f(x)$ and b_n is

$$b_n = B_1(\alpha^6)^n + B_2(\alpha^5)^n + B_3(\alpha^3)^n$$

For the initial vector ($b_0 = 0$, $b_1 = 1$, $b_2 = 1$)

$$\begin{cases} B_1 + B_2 + B_3 = 0 \\ \alpha^6 B_1 + \alpha^5 B_2 + \alpha^3 B_3 = 1 \\ \alpha^5 B_1 + \alpha^3 B_2 + \alpha^6 B_3 = 1 \end{cases}$$

We have $B_1 = \alpha, B_2 = \alpha^2, B_3 = \alpha^4$ and the general term of the sequence $\{b_n\}$ is

$$b_n = \alpha(\alpha^6)^n + \alpha^2(\alpha^5)^n + \alpha^4(\alpha^3)^n \tag{21}$$

 DOI: https://doi.org/10.30564/jeisr.v3i1.3507

The sequence $\{b_n\}$is periodic with the period $2^3-1=7$ and it is the flowing sequence

0 1 1 1 0 1 0, 0 1 1 1 0 ….

Figure 2 showing register generating $\{b_n\}$

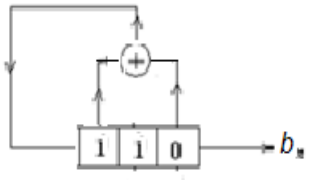

Figure 2. shift register generating $\{b_n\}$

We can look that one period of the sequence $\{b_n\}$is one period of the sequence $\{a_n\}$but through reading it by inverse from the right to the left.

Suppose the multiplication sequence $\{z_n\}$, where $z_n = a_n.b_n$, we have

$$z_n = a_n.b_n = \left[\alpha^2(\alpha)^n + \alpha^4(\alpha^2)^n + \alpha(\alpha^4)^n\right]$$
$$\left[\alpha(\alpha^6)^n + \alpha^2(\alpha^5)^n + \alpha^4(\alpha^3)^n\right] \quad (22)$$
$$z_n = a_n.b_n = \alpha^5\alpha^n + \alpha^3\alpha^{2n} + \alpha^2\alpha^{3n} + \alpha^6\alpha^{4n} +$$
$$\alpha\alpha^{5n} + \alpha^4\alpha^{6n} + 1$$

Thus, the sequence $\{z_n\}$ is a linear nonhomogeneous sequence with the length of its linear equivalent is equals 6 that is equal to $(\deg f(x))^2 - \deg f(x) = 6$, The period of $\{z_n\}$is 7, and the sequence $\{a_n\}$ is

0101010, 0101010 …….

We can check that the set of the all periodic permutation of one period is not an orthogonal set for example , for one permutation of the period: 0101010 is: 0010101 and the sum of the two vectors is 0111111.

Suppose the linear homogeneous part of zn is $LHP(z_n) = \{z_n'\}$;

$$LHP(z_n) = z_n' = \alpha^5\alpha^n + \alpha^3\alpha^{2n} + \alpha^2\alpha^{3n} + \alpha^6\alpha^{4n}$$
$$+ \alpha\alpha^{5n} + \alpha^4\alpha^{6n} \quad (23)$$

The sequence $\{z_n'\}$ is

1 0 1 0 1 0 1, 1 0 1 0 1 0 1 …

As the sequence $\{z_n\}$ the set of all periodic permutations of one period of the sequence $\{z_n'\}$is not an orthogonal set.

Figure 3, illustrates the linear feedback shift registers generating the sequence $\{z_n\}$.

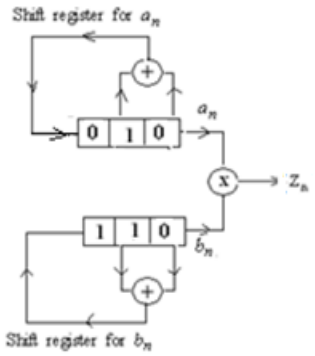

Figure 3. Illustrated the multiplication sequence $\{z_n\}$

We can look that $\alpha^n.\alpha^{2n}.\alpha^{3n}.\alpha^{4n}.\alpha^{5n}.\alpha^{6n} = \alpha^{21n} = 1$, and the characteristic equation of the sequence $\{z_n'\}$is of the form

$$x^6 + \mu_5x^5 + \mu_4x^4 + +\mu_3x^3 + \mu_2x^2 + \mu_1x + 1 = 0$$

Or

$$z'_{n+6} + \mu_5z'_{n+5} + \mu_4z'_{n+4} + \mu_3z'_{n+3} + \mu_2z'_{n+2} + \mu_1z'_{n+1} + z'_n = 0$$

Thus, for n = 0,1,2,3,4,5 we have the following system of equations

$$\begin{cases} 1+\mu_4+\mu_2+1=0 \\ 1+\mu_5+\mu_3+\mu_1=0 \\ \mu_5+\mu_4+\mu_2+1=0 \\ 1+\mu_4+\mu_3+\mu_1=0 \\ \mu_5+\mu_3+\mu_2+1=0 \end{cases}$$

Solving this system we have: $\mu_5=\mu_4=\mu_3=\mu_2=\mu_1=1$ and the characteristic equation of the sequence $\{z_n'\}$is

$$x^6 + x^5 + x^4 + x^3 + x^2 + x + 1 = 0 \quad (24)$$

Or

$$(x^3 + x + 1)(x^3 + x^2 + 1) = 0$$

And the recurring formula of the sequence $\{z_n'\}$is

$$z'_{n+6} + z'_{n+5} + z'_{n+4} + z'_{n+3} + z'_{n+2} + z'_{n+1} + z'_n = 0 \quad (25)$$

Figure4 showing the linear equivalent of the $\{z_n'\}$:

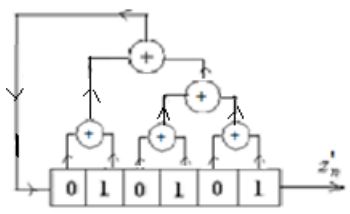

Figure 4. the linear feedback shift register generating the sequence $\{z_n'\}$

We can get $\{z_n\}$ from $\{z_n'\}$ by adding complement gate at the output of $\{z_n'\}$.

DOI: https://doi.org/10.30564/jeisr.v3i1.3507

Example 2

Giving the sequence $\{a_n\}$ generating by shift register as in Figure 5.

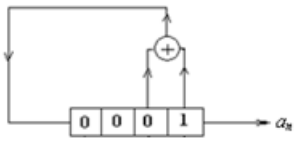

Figure 5. Linear feedback shift register generating sequence $\{a_n\}$

Where

$$a_{n+4} + a_{n+1} + a_n = 0 \text{ or } a_{n+4} = a_{n+1} + a_n \quad (26)$$

And $f(x) = x^4 + x + 1$ is its prime characteristic polynomial with the roots $\beta, \beta^2, \beta^4 = \beta + 1, \beta^8 = \beta^2 + 1$ which are lie in the field F_{2^4} where

$$F_{2^4} = \{0, \beta, \beta^2, \beta^3, \beta^4 = \beta + 1, \beta^5 = \beta^2 + \beta, \beta^6 = \beta^3 + \beta^2,$$
$$\beta^7 = \beta^3 + \beta + 1, \beta^8 = \beta^2 + 1, \beta^9 = \beta^3 + \beta,$$
$$\beta^{10} = \beta^2 + \beta + 1, \beta^{11} = \beta^3 + \beta^2 + \beta, \beta^{12} = \beta^3 + \beta^2 + \quad (27)$$
$$\beta + 1, \beta^{13} = \beta^3 + \beta^2 + 1, \beta^{14} = \beta^3 + 1, \beta^{15} = 1\}$$

And a_n is of the form

$$a_n = A_1\beta^n + A_2\beta^{2n} + A_3\beta^{4n} + A_4\beta^{8n}$$

Or

$$a_n = A_1\beta^n + A_2\beta^{2n} + A_3(\beta + 1)^n + A_4(\beta^2 + 1)^n$$

The periodic of the sequence $\{a_n\}$ is 2^4-1 = 15 and

$$n = 0 \Rightarrow A_1 + A_2 + A_3 + A_4 = 1$$
$$n = 1 \Rightarrow A_1\beta + A_2\beta^2 + A_3\beta^4 + A_4\beta^8 = 0$$
$$n = 2 \Rightarrow A_1\beta^2 + A_2\beta^4 + A_3\beta^8 + A_4\beta^{16} = 0$$
$$n = 3 \Rightarrow A_1\beta^3 + A_2\beta^6 + A_3\beta^{12} + A_4\beta^{24} = 0$$

Or

$$\begin{cases} A_1 + A_2 + A_3 + A_4 = 1 \\ A_1\beta + A_2\beta^2 + A_3(\beta + 1) + A_4(\beta^2 + 1) = 0 \\ A_1\beta^2 + A_2(\beta + 1) + A_3(\beta^2 + 1) + A_4\beta = 0 \\ A_1\beta^3 + A_2(\beta^3 + \beta^2) + A_3(\beta^3 + \beta^2 + \beta + 1) + A_4(\beta^3 + \beta) = 0 \end{cases}$$

Solution this system gives us

$$A_1 = \beta^{14}, A_2 = \beta^{13}, A_3 = \beta^{11}, A_4 = \beta^7$$

And

$$a_n = \beta^{14}(\beta)^n + \beta^{13}(\beta^2)^n + \beta^{11}(\beta^4)^n + \beta^7(\beta^8)^n \quad (28)$$

And $\{a_n\}$ is a M-Sequence with period 2^4-1 = 15.

100010011010111 100010011010111 ..... (29)

The cyclic permutations of one period form an orthogonal set.

The sequence $b_{n+4} + b_{n+3} + b_n = 0$ or $b_{n+4} = b_{n+3} + b_n$ is recurring and $g(x) = x^4 + x^3 + 1$ is its characteristic polynomial is prime and reciprocal $f(x)$, and

$$\beta_1 = \frac{\beta^{15}}{\beta} = \beta^{14}, \beta_2 = \frac{\beta^{15}}{\beta^2} = \beta^{13}, \beta_3 = \frac{\beta^{15}}{\beta^4} = \beta^{11}, \beta_3 = \frac{\beta^{15}}{\beta^8} = \beta^7$$

Are roots of $g(x)$ and b_n is

$$b_n = B_1(\beta^{14})^n + B_2(\beta^{13})^n + B_3(\beta^{11})^n + B_4(\beta^7)^n$$

For the initial vector (b_n= 0, b_1 = 1, b_2 = 1, b_3 = 1)

$$\begin{cases} n = 0 \Rightarrow B_1 + B_2 + B_3 + B_4 = 0 \\ n = 1 \Rightarrow \beta^{14}B_1 + \beta^{13}B_2 + \beta^{11}B_3 + \beta^7 B_4 = 1 \\ n = 2 \Rightarrow \beta^{13}B_1 + \beta^{11}B_2 + \alpha^7 B_3 + \beta^{14}B_4 = 1 \\ n = 3 \Rightarrow \beta^{12}B_1 + \beta^9 B_2 + \beta^3 B_3 + \beta^6 B_4 = 1 \end{cases}$$

We have $B_1 = B_2 = B_3 = B_4 = 1$, and b_n is

$$b_n = (\beta^{14})^n + (\beta^{13})^n + (\beta^{11})^n + (\beta^7)^n \quad (30)$$

The period of $\{b_n\}$ is 2^4 — 1=15 and the sequence is

0 1 1 1 1 0 1 0 1 1 0 0 1 0 0, 0 1 1 1 1 0 1 0 1 1 0 0 1 0 0 …. (31)

For the initial vector (1 1 1 0) we have the sequence $\{b_n^{'}\}$ where, we can get the general term of $\{b_n^{'}\}$ from b_n through shifting n by 2 and $b_n^{'}$ is

$$b_n^{'} = \beta^{13}(\beta^{14})^n + \beta^{11}(\beta^{13})^n + \beta^7(\beta^{11})^n + \beta^{14}(\beta^7)^n \quad (32)$$

And the sequence $\{b_n^{'}\}$ is

1 1 1 0 1 0 1 1 0 0 1 0 0 0 1, 1 1 1 0 1 0 1 1 0 0 1 0 0 0 1, 1 1 1 …. (33)

Figure 6 showing the linear feedback shift register generating $\{b_n\}$

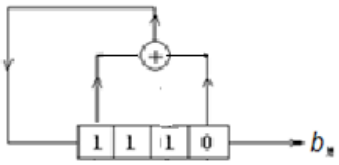

Figure 6. Shift register generating $\{b_n\}$

We can look that one period of the sequence $\{b_n\}$ is one period of the sequence $\{a_n\}$ but by reading it by inverse from the right to the left.

Suppose the multiplication sequence $\{z_n\}$ where $z_n = a_n.b_n$ we have

$$z_n = a_n.b_n = [\beta^{14}.\beta^n + \beta^{13}.\beta^{2n} + \beta^{11}.\beta^{4n} + \beta^7.\beta^{8n}]$$
$$[(\beta^{14})^n + (\beta^{13})^n + (\beta^{11})^n + (\beta^7)^n] \quad (34)$$
$$z_n = \beta^{14}\beta^{14n} + \beta^{13}\beta^{13n} + \beta^{14}\beta^{12n} + \beta^{12}\beta^{11n} + \beta^{13}\beta^{9n} + \beta^{14}\beta^{8n}$$
$$+ \beta^7\beta^{7n} + \beta^7\beta^{6n} + \beta^7\beta^{4n} + \beta^{12}\beta^{3n} + \beta^{12}\beta^{2n} + \beta^{13}\beta^n$$

Thus, the sequence $\{z_n\}$ is a linear homogeneous sequence with the length 12 and equal to $(\deg f(x))^2 -$ deg $f(x)$ =12, periodic with the period 15 and this sequence is

 DOI: https://doi.org/10.30564/jeisr.v3i1.3507

100010010010001, 100010010010001, 10001 …

We can check that the set of the all periodic permutations of one period of $\{z_n\}$ is not orthogonal set.

Figure 7 illustrated the nonlinear feedback shift register generating $\{z_n\}$.

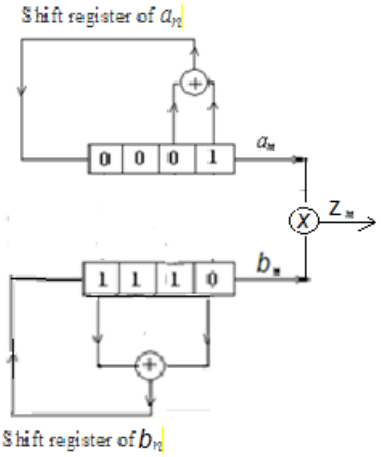

Figure 7. Illustrated the multiplication sequence $\{z_n\}$

We can look that $\beta^{14n}.\beta^{13n}.\beta^{12n}..\beta^{11n}\beta^{9n}\beta^{8n}\beta^{7n}\beta^{6n}\beta^{4n}\beta^{3n}\beta^{2n}\beta^{n}=\beta^{90n}=1$.

Thus, the characteristic equation of $\{z_n'\}$ is of the form;

$$x^{12}+\mu_{11}x^{11}+\mu_{10}x^{10}+\mu_9x^9+\mu_8x^8+\mu_7x^7+\mu_6x^6+\mu_5x^5+\mu_4x^4+\mu_3x^3+\mu_2x^2+\mu_1x+1=0$$

Or

$$z_{n+16}+\mu_{11}z_{n+11}+\mu_{10}z_{n+10}+\mu_9z_{n+9}+\mu_8z_{n+8}+\mu_7z_{n+7}+\mu_6z_{n+6}+\mu_5z_{n+5}+\mu_4z_{n+4}+\mu_3z_{n+3}+\mu_2z_{n+2}+\mu_1z_{n+1}+z_n=0$$

Thus, for n = 0,1,2,3,…,10 and adding for $n = 11$ because the equation for $n = 10$ is linearly pending with the equations for $n = 0$ to $n = 9$ we have the following system of 12 equations:

$$\begin{cases}\mu_{10}+\mu_7+\mu_4=1\\ \mu_9+\mu_6+\mu_3=0\\ \mu_8+\mu_5+\mu_2=1\\ \mu_{11}+\mu_7+\mu_4+\mu_1=1\end{cases}$$

$$\begin{cases}\mu_{11}+\mu_{10}+\mu_6+\mu_3=1\\ \mu_{10}+\mu_9+\mu_5+\mu_2=0\\ \mu_9+\mu_8+\mu_4+\mu_1=0\\ \mu_8+\mu_7+\mu_3=0\end{cases}$$

$$\begin{cases}\mu_{11}+\mu_7+\mu_6+\mu_2=0\\ \mu_{10}+\mu_6+\mu_5+\mu_1=0\\ \mu_9+\mu_5+\mu_4=0\\ \mu_{11}+\mu_8+\mu_4+\mu_3=0\end{cases}$$

Solving this system we have: $\mu_{11}=\mu_9=\mu_8=\mu_2=0$; $\mu_{10}=\mu_7=\mu_6=\mu_5=\mu_4=\mu_3=\mu_1=1$ and the characteristic equation of the sequence $\{z_n\}$ is

$$x^{12}+x^{10}+x^7+x^6+x^5+x^4+x^3+x+1=0 \quad (35)$$

And the recurring formula of the sequence $\{z_n\}$ is

$$z_{n+12}+z_{n+10}+z_{n+7}+z_{n+6}+z_{n+5}+z_{n+4}+z_{n+3}+z_{n+1}+z_n=0 \quad (36)$$

Figure 8 showing the linear equivalent of the $\{z_n\}$:

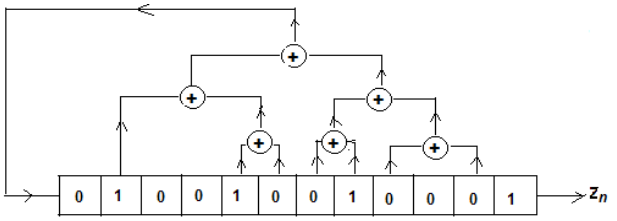

Figure 8. Shift register generating sequence $\{z_n\}$

Example 3

Given in Figure 9 the shift register generating the recurring sequence $\{a_n\}$ with five degrees:

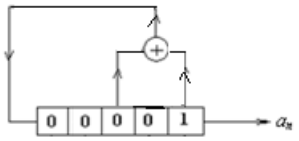

Figure 9. Shift register generating the sequence $\{a_n\}$

Where

$$a_{n+5}+a_{n+2}+a_n=0 \text{ or } a_{n+5}=a_{n+2}+a_n \quad (37)$$

And $\{a_n\}$ has the polynomial $f(x)=x^5+x^2+1$ as a prime characteristic polynomial, the roots $f(x)$ are; $\gamma,\gamma^2,\gamma^4,\gamma^8=\gamma^3+\gamma^2+1,\gamma^{16}=\gamma^4+\gamma^3+\gamma+1$ which are lie in the field F_{2^5} and

$$F_{2^5}=\{0,\gamma,\gamma^2,\gamma^3,\gamma^4,\gamma^5=\gamma^2+1,\gamma^6=\gamma^3+\gamma,\gamma^7=\gamma^4+\gamma^2,\gamma^8=\gamma^3+\gamma^2+1,\gamma^9=\gamma^4+\gamma^3+\gamma,\gamma^{10}=\gamma^4+1,\ \gamma^{11}=\gamma^2+\gamma+1,\gamma^{12}=\gamma^3+\gamma^2+\gamma,\gamma^{13}=\gamma^4+\gamma^3+\gamma^2,\gamma^{14}=\gamma^4+\gamma^3+\gamma^2+1,\gamma^{15}=\gamma^4+\gamma^3+\gamma^2+\gamma+1,\ \gamma^{16}=\gamma^4+\gamma^3+\gamma+1,\gamma^{17}=\gamma^4+\gamma+1,\gamma^{18}=\gamma+1,\gamma^{19}=\gamma^2+\gamma,\gamma^{20}=\gamma^3+\gamma^2,\gamma^{21}=\gamma^4+\gamma^3,\ \gamma^{22}=\gamma^4+\gamma^2+1,\gamma^{23}=\gamma^3+\gamma^2+\gamma+1,\gamma^{24}=\gamma^4+\gamma^3+\gamma^2+\gamma,\gamma^{25}=\gamma^4+\gamma^3+1,\gamma^{26}=\gamma^4+\gamma^2+\gamma+1,\ \gamma^{27}=\gamma^3+\gamma+1,\gamma^{28}=\gamma^4+\gamma^2+\gamma,\gamma^{29}=\gamma^3+1,\gamma^{30}=\gamma^4+\gamma,\gamma^{31}=1\}$$

And a_n of the form

$$a_n=A_1\gamma^n+A_2\gamma^{2n}+A_3\gamma^{4n}+A_4\gamma^{8n}+A_5\gamma^{16n}$$

Or

$$a_n=A_1\beta^n+A_2(\gamma^2)^n+A_3(\gamma^4)^n+A_4(\gamma^3+\gamma^2+1)^n+A_5(\gamma^4+\gamma^3+\gamma+1)^n$$

DOI: https://doi.org/10.30564/jeisr.v3i1.3507

And

$$n=0 \Rightarrow A_1+A_2+A_3+A_4+A_5=1$$
$$n=1 \Rightarrow A_1\gamma+A_2\gamma^2+A_3\gamma^4+A_4\gamma^8+A_5\gamma^{16}=0$$
$$n=2 \Rightarrow A_1\gamma^2+A_2\gamma^4+A_3\gamma^8+A_4\gamma^{16}+A_5\gamma=0$$
$$n=3 \Rightarrow A_1\gamma^3+A_2\gamma^6+A_3\gamma^{12}+A_4\gamma^{24}+A_5\gamma^{17}=0$$
$$n=4 \Rightarrow A_1\gamma^4+A_2\gamma^8+A_3\gamma^{16}+A_4\gamma+A_5\gamma^2=0$$

From the previously system of equation we have

$$A_1=\gamma^{26}, A_2=\gamma^{21}, A_3=\gamma^{11}, A_4=\gamma^{22}, A_5=\gamma^{13}$$

Thus, a_n is equals

$$a_n=\gamma^{26}.(\gamma)^n+\gamma^{21}.(\gamma^2)^n+\gamma^{11}.(\gamma^4)^n+\gamma^{22}.(\gamma^8)^n+\gamma^{13}(\gamma^{16})^n \quad (39)$$

The period of $\{a_n\}$is 2^5-1 = 31, and the all cyclic permutations of one period is an orthogonal set.

1 0 0 0 0 1 0 0 1 0 1 1 0 0 1 1 1 1 1 0 0 0 1 1 0 1 1 1 0 1 0 1 0 0 0 0 1 0 …… (40)

Suppose the binary recurring sequence $b_{n+5}+b_{n+3}+b_n=0$ or $b_{n+5}=b_{n+3}+b_n$ with the prime characteristic polynomial $g(x)=x^5+x^3+1$ which is the reciprocal $f(x)$, thus the roots of $g(x)$ are

$$\gamma_1=\frac{\gamma^{31}}{\gamma}=\gamma^{30}, \gamma_2=\frac{\gamma^{31}}{\gamma^2}=\gamma^{29}, \gamma_3=\frac{\gamma^{31}}{\gamma^4}=\gamma^{27},$$
$$\gamma_4=\frac{\gamma^{31}}{\gamma^8}=\gamma^{23}, \gamma_5=\frac{\gamma^{31}}{\gamma^{16}}=\gamma^{15}$$

Is very easy looking that $\gamma^{30}, \gamma^{29}, \gamma^{27}, \gamma^{23}, \gamma^{15}$ are roots of the characteristic polynomial $g(x)$ and the b_n is of the form

$$b_n=B_1(\gamma^{30})^n+B_2(\gamma^{29})^n+B_3(\gamma^{27})^n+B_4(\gamma^{23})^n+B_5(\gamma^{15})^n$$

For the initial vector ($b_n=0, b_1=1, b_2=0, b_3=1, b_4=1$, are the latest 5th values of one period of the sequence $\{a_n\}$ but by inverse we read them from the right to the left) and by solving the following system for n = 0, n =1, n = 2, 3 and n = 4)

$$\begin{cases} B_1+B_2+B_3+B_4+B_5=0 \\ \gamma^{30}B_1+\gamma^{29}B_2+\gamma^{27}B_3+\gamma^{23}B_4+\gamma^{15}B_4=1 \\ \gamma^{29}B_1+\gamma^{27}B_2+\gamma^{23}B_3+\gamma^{15}B_4+\gamma^{30}B_4=0 \\ \gamma^{28}B_1+\gamma^{25}B_2+\gamma^{19}B_3+\gamma^{7}B_4+\gamma^{14}B_4=1 \\ \gamma^{27}B_1+\gamma^{23}B_2+\gamma^{15}B_3+\gamma^{30}B_4+\gamma^{29}B_4=1 \end{cases}$$

Solving this system of equations we have: $B_1=\gamma^{25}$, $B_2=\gamma^{19}, B_3=\gamma^7, B_4=\gamma^{14}, B_5=\gamma^{28}$, and b_n is

$$b_n=\gamma^{25}(\gamma^{30})^n+\gamma^{19}(\gamma^{29})^n+\gamma^7(\gamma^{27})^n+\gamma^{14}(\gamma^{23})^n+\gamma^{28}(\gamma^{15})^n \quad (41)$$

The sequence $\{b_n\}$is periodic with the period $2^5-1=$ 31 and it is the flowing sequence:

0 1 0 1 1 1 0 1 1 0 0 0 1 1 1 1 1 0 0 1 1 0 1 0 0 1 0 0 0 0 1, 0101110 … (42)

Figure 10 illustrated shift register generating $\{b_n\}$.

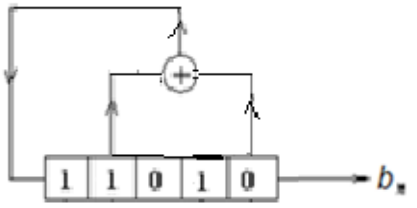

Figure 10. Shift register generating sequence$\{b_n\}$

We can look that one period of the sequence $\{b_n\}$is an one period of the sequence $\{a_n\}$but by reading it by inverse from the right to the left.

Suppose the multiplication sequence $\{z_n\}$ where $z_n=a_n.b_n$, we have

$$z_n=a_n.b_n$$
$$=\left[\gamma^{26}.(\gamma)^n+\gamma^{21}.(\gamma^2)^n+\gamma^{11}.(\gamma^4)^n+\gamma^{22}.(\gamma^8)^n+\gamma^{13}(\gamma^{16})^n\right]\left[\gamma^{25}(\gamma^{30})^n+\gamma^{19}(\gamma^{29})^n+\gamma^7(\gamma^{27})^n+\gamma^{14}(\gamma^{23})^n+\gamma^{28}(\gamma^{15})^n\right]$$

$$\begin{aligned} z_n=&\gamma^{15}\gamma^n+\gamma^{30}\gamma^{2n}+\gamma^5\gamma^{3n}+\gamma^{29}\gamma^{4n}+\gamma^{10}\gamma^{6n}+\\ &\gamma^{16}\gamma^{7n}+\gamma^{27}\gamma^{8n}+\gamma^{20}\gamma^{12n}+\gamma\ \gamma^{14n}+\gamma^7\lambda^{15n}+\\ &\gamma^{23}\gamma^{16n}+\gamma^{18}\gamma^{17n}+\gamma^8\gamma^{19n}+\gamma^{19}\gamma^{23n}+\gamma^9\gamma^{24n}+\\ &\gamma^4\gamma^{25n}+\gamma^{25}\gamma^{27n}+\gamma^2\gamma^{28n}+\gamma^{28}\gamma^{29n}+\gamma^{14}\gamma^{30n}+\\ &(\gamma^{20}+\gamma^9+\gamma^{18}+\gamma^5+\gamma^{10}) \end{aligned} \quad (43)$$

$$\begin{aligned} z_n=&\gamma^{15}\gamma^n+\gamma^{30}\gamma^{2n}+\gamma^5\gamma^{3n}+\gamma^{29}\gamma^{4n}+\gamma^{10}\gamma^{6n}+\\ &\gamma^{16}\gamma^{7n}+\gamma^{27}\gamma^{8n}+\gamma^{20}\gamma^{12n}+\gamma\ \gamma^{14n}+\gamma^7\lambda^{15n}+\\ &\gamma^{23}\gamma^{16n}+\gamma^{18}\gamma^{17n}+\gamma^8\gamma^{19n}+\gamma^{19}\gamma^{23n}+\gamma^9\gamma^{24n}+\\ &\gamma^4\gamma^{25n}+\gamma^{25}\gamma^{27n}+\gamma^2\gamma^{28n}+\gamma^{28}\gamma^{29n}+\gamma^{14}\gamma^{30n}+1 \end{aligned}$$

Thus, the sequence $\{z_n\}$ is a linear nonhomogeneous sequence and it is:

0 0 0 0 0 1 0 0 1 0 0 0 0 0 1 1 1 0 0 0 0 0 1 0 0 1 0 0 0 0 0, 0000010 ……. (44)

The set of all cyclic permutations of one period is not orthogonal set.

Suppose the linear homogeneous part with the sequence is $\{z'_n\}$, which it's linear equivalent has the length $(\deg f(x))^2-\deg f(x)=20$, and the period of $\{z'_n\}$is 31 and $\{z'_n\}$is the complement of e $\{z_n\}$, thus, $\{z_n\}$is

1 1 1 1 1 0 1 1 0 1 1 1 1 1 1 0 0 0 1 1 1 1 1 0 1 1 0 1 1 1 1 1, 1111101 …….. (45)

And the set of the all cyclic permutations of one period of $\{z_n\}$is not an orthogonal set. Figure 11 shows the nonlinear shift register generating the sequence $\{z_n\}$.

 DOI: https://doi.org/10.30564/jeisr.v3i1.3507

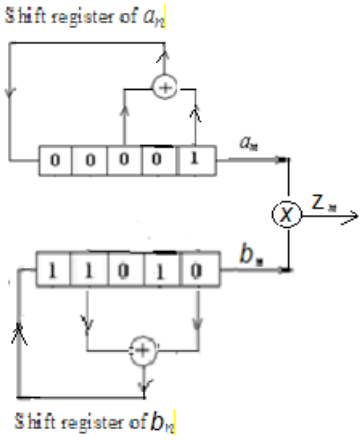

Figure11. Illustrated the multiplication sequence $\{z_n\}$

According with the sequences $\{a_n\}$, its reciprocal sequence $\{b_n\}$ and their multiplication sequence $\{z_n\}$ in the examples 1, 2, 3 we have

$$\text{In example 1: } \begin{cases} a_n = \alpha^2(\alpha)^n + \alpha^4(\alpha^2)^n + \alpha(\alpha^4)^n \\ b_n = \alpha(\alpha^6)^n + \alpha^2(\alpha^5)^n + \alpha^4(\alpha^3)^n \end{cases} \quad (46)$$

In example 2:

$$\begin{cases} a_n = \beta^{14}.(\beta)^n + \beta^{13}.(\beta^2)^n + \beta^{11}.(\beta^4)^n + \beta^7.(\beta^8)^n \\ b_n^{'} = \beta^{13}(\beta^{14})^n + \beta^{11}(\beta^{13})^n + \beta^7(\beta^{11})^n + \beta^{14}(\beta^7)^n \end{cases} \quad (47)$$

In example 3:

$$\begin{cases} a_n = \gamma^{26}.(\gamma)^n + \gamma^{21}.(\gamma^2)^n + \gamma^{11}.(\gamma^4)^n + \gamma^{22}.(\gamma^8)^n \\ \quad + \gamma^{13}(\gamma^{16})^n \\ b_n = \gamma^{25}(\gamma^{30})^n + \gamma^{19}(\gamma^{29})^n + \gamma^7(\gamma^{27})^n + \gamma^{14}(\gamma^{23})^n \\ \quad + \gamma^{28}(\gamma^{15})^n \end{cases} \quad (48)$$

We can look the following properties

*P*1. For one period of the sequence $\{a_n\}$ the period of its reciprocal sequence $\{b_n\}$ is the same but must read or write it by inverse from the right to the left.

*P*2. In the both form of the general term of each of them and for two consecutive coefficients in each of them the square of the first coefficient equals the second coefficient, namely; $(A_i)^2 = A_{i+1}$, $(B_i)^2 = B_{i+1}$ and the square of the first term equals the second term .

*P*3. The exponent of the coefficient of the first term in the general term in the sequence $\{a_n\}$ is larger than the corresponding coefficient in the sequence$\{b_n\}$ by one.

*P*4. The length of the linear homogeneous part of the sequence $\{z_n\}$is equal to $((\deg f(x))^2 - \deg f(x))$ Where the $f(x)$ is the characteristic polynomial of the sequence$\{a_n\}$.

we will check these four properties by studying the case when the degree of the prime characteristic function of the sequence $\{a_n\}$ is six where

$$a_{n+6} + a_{n+1} + a_n = 0 \cdots or\ a_{n+6} = a_{n+1} + a_n \quad (49)$$

Where

$$f(x) = x^6 + x + 1 \quad (50)$$

The characteristic equation is

$$x^6 + x + 1 = 0 \quad (51)$$

If α is a root of the characteristic equation then α generates the field $F2^6$, where Appendix1 showing the elements of this field.

The term a_n is

$$a_n = A_1\alpha^n + A_2\alpha^{2n} + A_3\alpha^{4n} + A_4\alpha^{8n} + A_5\alpha^{16n} + A_6\alpha^{32n}$$

And

$$n = 0 \Rightarrow A_1 + A_2 + A_3 + A_4 + A_5 + A_6 = 1$$
$$n = 1 \Rightarrow A_1\alpha + A_2\alpha^2 + A_3\alpha^4 + A_4\alpha^8 + A_5\alpha^{16} + A_6\alpha^{32} = 0$$
$$n = 2 \Rightarrow A_1\alpha^2 + A_2\alpha^4 + A_3\alpha^8 + A_4\alpha^{16} + A_5\alpha^{32} + A_6\alpha = 0$$
$$n = 3 \Rightarrow A_1\alpha^3 + A_2\alpha^6 + A_3\alpha^{12} + A_4\alpha^{24} + A_5\alpha^{48} + A_6\alpha^{33} = 0$$
$$n = 4 \Rightarrow A_1\alpha^4 + A_2\alpha^8 + A_3\alpha^{16} + A_4\alpha^{32} + A_5\alpha + A_6\alpha^2 = 0$$
$$n = 5 \Rightarrow A_1\alpha^5 + A_2\alpha^{10} + A_3\alpha^{20} + A_4\alpha^{40} + A_5\alpha^{17} + A_6\alpha^{34} = 0$$

Or, using Gaussian methods

$$A_1 + A_2 + A_3 + A_4 + A_5 + A_6 = 1$$
$$A_2 + A_3\alpha^{26} + A_4\alpha^{20} + A_5\alpha^{17} + A_6\alpha^{28} = \alpha^{57}$$
$$A_3 + A_4\alpha^{46} + A_5\alpha^{31} + A_6\alpha^{36} = \alpha^{19}$$
$$A_4 + A_5\alpha^{26} + A_6\alpha^7 = \alpha^{12}$$
$$A_5 + A_6 = \alpha$$
$$A_6\alpha^{17} = \alpha^{48}$$

Thus

$$A_6 = \alpha^{31}$$

According with the property P_2 we can guess $A_1,\ldots, A_5$, as the following

$$A_5 = (A_6)^{1/2} = (\alpha^{31})^{1/2} = (\alpha^{31+63})^{1/2} = \alpha^{47}$$
$$A_4 = (A_5)^{1/2} = (\alpha^{47})^{1/2} = (\alpha^{47+63})^{1/2} = \alpha^{55}$$
$$A_3 = (A_4)^{1/2} = (\alpha^{55})^{1/2} = (\alpha^{55+63})^{1/2} = \alpha^{59}$$
$$A_2 = (A_3)^{1/2} = (\alpha^{59})^{1/2} = (\alpha^{59+63})^{1/2} = \alpha^{61}$$
$$A_1 = (A_2)^{1/2} = (\alpha^{61})^{1/2} = (\alpha^{61+63})^{1/2} = \alpha^{62}$$

We can check these results through solving the above system of equations and we have the same results.

Thus, the term *a*n is

$$a_n = \alpha^{62}\alpha^n + \alpha^{61}\alpha^{2n} + \alpha^{59}\alpha^{4n} + \alpha^{55}\alpha^{8n} + \alpha^{47}\alpha^{16n} + \alpha^{31}\alpha^{32n} \quad (52)$$

The sequence $\{a_n\}$ is M-Sequence, periodic with the period 2^6-1 = 63, and the all cyclic permutations of one period is an orthogonal set and the sequence is

DOI: https://doi.org/10.30564/jeisr.v3i1.3507

1000001000. 0110001010. 0111101000. 1110010010. 1101110110. 0110101011.111, 1000 …. (53)

The reciprocal polynomial of $f(x)$ is $g(x) = x^6 + x^5 + 1$ and for the initial vector $(b_0b_1b_2b_3b_4b_5) = (111110)$ we have the following reciprocal sequence $\{b_n\}$

111.1101010110.0110111011.0100100111.0001011110.0101000110. 0001000001, 111110 …. (54)

By checking the general terms of the sequence $\{s_n\}$ where

$$s_n = B_1\alpha^{62n} + B_2\alpha^{61n} + B_3\alpha^{59n} + B_4\alpha^{55n} + B_5\alpha^{47n} + B_6\alpha^{31n}$$

Where α^{62} is reciprocal α, α^{62} is reciprocal α^2, …, α^{31} is reciprocal α^{32}.

According with property P_3 and P_2 we can guess B_1,…, B_6, as the following

$$B_1 = \alpha^{62-1} = \alpha^{61}$$
$$B_2 = (B_1)^2 = (\alpha^{61})^2 = \alpha^{122} = \alpha^{59}$$
$$B_3 = (B_2)^2 = (\alpha^{59})^2 = \alpha^{118} = \alpha^{55}$$
$$B_4 = (B_3)^2 = (\alpha^{55})^2 = \alpha^{110} = \alpha^{37}$$
$$B_5 = (B_4)^2 = (\alpha^{37})^2 = \alpha^{74} = \alpha^{11}$$
$$B_6 = (B_5)^2 = (\alpha^{11})^2 = \alpha^{22} = \alpha^{22}$$

And thus; the suggested general term of the sequence $\{s_n\}$ is

$$s_n = \alpha^{61}\alpha^{62n} + \alpha^{59}\alpha^{61n} + \alpha^{55}\alpha^{59n} + \alpha^{37}\alpha^{55n} + \alpha^{11}\alpha^{47n} + \alpha^{22}\alpha^{31n}$$

We can check that the sequence $\{s_n\}$ is the same reciprocal sequence $\{b_n\}$ and thus

$$b_n = \alpha^{61}\alpha^{62n} + \alpha^{59}\alpha^{61n} + \alpha^{55}\alpha^{59n} + \alpha^{37}\alpha^{55n} + \alpha^{11}\alpha^{47n} + \alpha^{22}\alpha^{31n} \quad (55)$$

Thus

$$\begin{cases} a_n = \alpha^{62}\alpha^{n} + \alpha^{61}\alpha^{2n} + \alpha^{59}\alpha^{4n} + \alpha^{55}\alpha^{8n} + \alpha^{47}\alpha^{16n} + \alpha^{31}\alpha^{32n} \\ b_n = \alpha^{61}\alpha^{62n} + \alpha^{59}\alpha^{61n} + \alpha^{55}\alpha^{59n} + \alpha^{37}\alpha^{55n} + \alpha^{11}\alpha^{47n} + \alpha^{22}\alpha^{31n} \end{cases}$$

Also we can check that

$$a_n.b_n = \left(\sum_{i=1}^{6} A_i(\alpha^{2^{i-1}})^n\right)\left(\sum_{j=1}^{6} B_j(\alpha^{2^k-2^{j-1}-1})^n\right)$$
$$= \left(\sum_{i,j=1,i\neq j}^{6} A_iB_j(\alpha^{2^{i-1}}\alpha^{2^k-2^{j-1}-1})^n\right) + \sum_{i=1}^{6} A_iB_i$$

The first bracket contains 30 terms and

$$\sum_{i=1}^{6} A_iB_i = \alpha^{62}\alpha^{61} + \alpha^{61}\alpha^{59} + \alpha^{59}\alpha^{55} + \alpha^{55}\alpha^{37} + \alpha^{47}\alpha^{11} + \alpha^{31}\alpha^{22}$$
$$= \alpha^{123} + \alpha^{120} + \alpha^{114} + \alpha^{92} + \alpha^{58} + \alpha^{53}$$
$$= \alpha^{60} + \alpha^{57} + \alpha^{51} + \alpha^{39} + \alpha^{58} + \alpha^{53} = 1$$

Thus,

$$a_n.b_n = \left(\sum_{i,j=1,i\neq j}^{6} A_iB_j(\alpha^{2^{i-1}}\alpha^{2^k-2^{j-1}-1})^n\right) + 1$$

And the length of the linear equivalent of the linear homogeneous part of $a_n.b_n$ is equal to 30 that is equal to $((\deg f(x))^2 - \deg f(x))$.

4. Conclusions

For one period of the sequence $\{a_n\}$ the period of its reciprocal sequence $\{b_n\}$ is the same but we must read or write it by inverse from the right to the left.

In the both forms of the general term of the sequences $\{a_n\}$ and $\{b_n\}$ and for two consecutive coefficients in each of them the square of the first coefficient equals the second coefficient, namely; $(A_i)^2 = A_{i+1}$, $(B_i)^2 = B_{i+1}$ and the square of the first term is equals the second term.

The exponent of the coefficient of the first term in the general term in the sequence $\{a_n\}$ is larger than the corresponding coefficient in the first term of the sequence $\{b_n\}$ by one.

If each coefficient and its corresponding root (of the characteristic equation) in the general term of a sequence are reciprocal then these coefficients will be roots in the reciprocal sequence.

The length of the linear homogeneous part of the multiplication sequence $\{z_n\}$ is equals to $(\deg f(x))^2 - \deg f(x)$, where $f(x)$ is the prime characteristic polynomial of the sequence $\{a_n\}$.

The set of all cyclic permutations of one period of the reciprocal sequence $\{b_n\}$ is an orthogonal set but this set of the multiplication sequence $\{z_n\}$ is not an orthogonal set.

Each of the sequences $\{b_n\}$ and $\{z_n\}$ is a periodic sequence and has the same period of the sequence $\{a_n\}$.

References

[1] Sloane, N.J.A., (1976), "An Analysis Of The Stricture And Complexity of Nonlinear Binary Sequence Generators," *IEEE Trans. Information Theory* Vol. It 22 No 6, PP 732-736.

[2] Jong-Seon No, Solomon W. & Golomb, (1998), "Binary Pseudorandom Sequences For period 2^n-1 with Ideal Autocorrelation, *"IEEE Trans. Information*

Theory, Vol. 44 No 2, PP 814-817.

[3] Golamb S. W. (1976), Shift Register Sequences, San Francisco – Holden Day.

[4] Lee J.S &Miller L.E, (1998), "*CDMA System Engineering Hand Book, "*Artech House. Boston, London.

[5] Yang S.C,"*CDMA RF* , (1998), *System Engineering,"*Artech House. Boston- London.

[6] Yang K , Kg Kim y Kumar l. d, (2000), "Quasi–orthogonal Sequences for code –Division Multiple Access Systems, "*IEEE Trans .information theory*, Vol. 46, No3, PP 982-993.

[7] Mac Wiliams, F. G & Sloane,N.G.A., (2006), "*The Theory of Error- Correcting Codes,"* North-Holland, Amsterdam.

[8] Kasami, T. & Tokora, H., (1978), "Teoria Kodirovania, " *Mir*(*Moscow*).

[9] Al Cheikha. A. H., (2020), "Study the Linear Equivalent of the Binary Nonlinear Sequences". *International Journal of Information and Communication Sciences*. Vol. 5, No. 3, 2020, pp. 24-39.

[10] Al Cheikha A. H. (May 2014), "Matrix Representation of Groups in the finite Fields GF(*pn*)"International Journal of Soft Computing and Engineering, Vol. 4, Issue 2, PP 118-125.

[11] Lidl, R.& Pilz, G., (1984), "*Applied Abstract Algebra*," Springer – Verlage New York, 1984.

[12] Lidl, R. & Niderreiter, H., (1994), "Introduction to Finite Fields and Their Application, " *Cambridge university* USA.

[13] Thomson W. Judson, (2013), "*Abstract Algebra: Theory and Applications*," Free Software Foundation.

[14] Fraleigh, J.B., (1971), "A First course In Abstract Algebra, *Fourth printing. Addison- Wesley publishing company* USA.

[15] David, J., (2008), "Introductory Modern Algebra, "*Clark University* USA.

Appendix

F_{2^6}		
0	$\alpha^{20}=\alpha^5+\alpha^4+\alpha^3+\alpha^2$	$\alpha^{41}=\alpha^4+\alpha^3+\alpha^2+1$
$\alpha^{63}=1$	$\gamma^{21}=\gamma^5+\gamma^4+\gamma^3+\gamma+1$	$\alpha^{42}=\alpha^5+\alpha^4+\alpha^3+\alpha$
α	$\alpha^{22}=\alpha^5+\alpha^4+\alpha^2+1$	$\alpha^{43}=\alpha^5+\alpha^4+\alpha^2+\alpha+1$
α^2	$\alpha^{23}=\alpha^5+\alpha^3+1$	$\alpha^{44}=\alpha^5+\alpha^3+\alpha^2+1$
α^3	$\alpha^{24}=\alpha^4+1$	$\alpha^{45}=\alpha^4+\alpha^3+1$
α^4	$\alpha^{25}=\alpha^5+\alpha$	$\alpha^{46}=\alpha^5+\alpha^4+\alpha$
α^5	$\alpha^{26}=\alpha^2+\alpha+1$	$\alpha^{47}=\alpha^5+\alpha^2+\alpha+1$
$\alpha^6=\alpha+1$	$\alpha^{27}=\alpha^3+\alpha^2+\alpha$	$\alpha^{48}=\alpha^3+\alpha^2+1$
$\alpha^7=\alpha^2+\alpha$	$\alpha^{28}=\alpha^4+\alpha^3+\alpha^2$	$\alpha^{49}=\alpha^4+\alpha^3+\alpha$
$\alpha^8=\alpha^3+\alpha^2$	$\alpha^{29}=\alpha^5+\alpha^4+\alpha^3$	$\alpha^{50}=\alpha^5+\alpha^4+\alpha^2$
$\alpha^9=\alpha^4+\alpha^3$	$\alpha^{30}=\alpha^5+\alpha^4+\alpha+1$	$\alpha^{51}=\alpha^5+\alpha^3+\alpha+1$
$\alpha^{10}=\alpha^5+\alpha^4$	$\alpha^{31}=\alpha^5+\alpha^2+1$	$\alpha^{52}=\alpha^4+\alpha^2+1$
$\alpha^{11}=\alpha^5+\alpha+1$	$\alpha^{32}=\alpha^3+1$	$\alpha^{53}=\alpha^5+\alpha^3+\alpha$
$\alpha^{12}=\alpha^2+1$	$\alpha^{33}=\alpha^4+\alpha$	$\alpha^{54}=\alpha^4+\alpha^2+\alpha+1$
$\alpha^{13}=\alpha^3+\alpha$	$\alpha^{34}=\alpha^5+\alpha^2$	$\alpha^{55}=\alpha^5+\alpha^3+\alpha^2+\alpha$
$\alpha^{14}=\alpha^4+\alpha^2$	$\alpha^{35}=\alpha^3+\alpha+1$	$\alpha^{56}=\alpha^4+\alpha^3+\alpha^2+\alpha+1$
$\alpha^{15}=\alpha^5+\alpha^3$	$\alpha^{36}=\alpha^4+\alpha^2+\alpha$	$\alpha^{57}=\alpha^5+\alpha^4+\alpha^3+\alpha^2+\alpha$
$\alpha^{16}=\alpha^4+\alpha+1$	$\alpha^{37}=\alpha^5+\alpha^3+\alpha^2$	$\alpha^{58}=\alpha^5+\alpha^4+\alpha^3+\alpha^2+\alpha+1$
$\alpha^{17}=\alpha^5+\alpha^2+\alpha$	$\alpha^{38}=\alpha^4+\alpha^3+\alpha+1$	$\alpha^{59}=\alpha^5+\alpha^4+\alpha^3+\alpha^2+1$
$\alpha^{18}=\alpha^3+\alpha^2+\alpha+1$	$\alpha^{39}=\alpha^5+\alpha^4+\alpha^2+\alpha$	$\alpha^{60}=\alpha^5+\alpha^4+\alpha^3+1$
$\alpha^{19}=\alpha^4+\alpha^3+\alpha^2+\alpha$	$\alpha^{40}=\alpha^5+\alpha^3+\alpha^2+\alpha+1$	$\alpha^{61}=\alpha^5+\alpha^4+1$; $\alpha^{62}=\alpha^5+1$

DOI: https://doi.org/10.30564/jeisr.v3i1.3507

BILINGUAL PUBLISHING CO.
Pioneer of Global Academics Since 1984

Journal of Electronic & Information Systems
https://ojs.bilpublishing.com/index.php/jeis

ARTICLE

Wireless Power Transfer for 6G Network Using Monolithic Components on GaN

Rajinikanth Yella[1*] Krishna Pande[2] Ke Horng Chen[2]

1. Electrical Engineering Computer Science (EECS), NCTU, Taiwan, China
2. Electrical Engineering (EE), NCTU, Taiwan, China

ARTICLE INFO

Article history
Received: 11 August 2021
Accepted: 20 August 2021
Published Online: 30 August 2021

Keywords:
Wireless power transfer
Antenna
Rectifier
Filter

ABSTRACT

A novel architecture for Wireless Power Transfer (WPT) module using monolithic components on GaN is presented in this paper. The design of such a WPT module receives DC power from solar panels, consists of photonic power converter (PPC), beamforming antenna, low pass filter, input matching network, rectifier, output matching network and logic circuit (off-chip) which are all integrated on a GaN chip. Our WPT components show excellent simulated performance, for example, our novel beam-forming antenna and multiple port wideband antenna have a gain of 8.7 dB and 7.3 dB respectively. We have added a band pass filter to the rectifier output which gives two benefits to the circuit. The first one is filtering circuit will remove unwanted harmonics before collecting DC power and second is filter will boost the efficiency of rectifier by optimizing the load impedance. Our proposed rectifier has RF-DC conversion efficiency of 74% and 67% with beam-forming antenna and multiple port wide band antenna respectively. Our WPT module is designed to charge a rechargeable battery (3 V and 1 mA) of a radio module which will be used between two antennas in future 5G networks. We believe our proposed WPT module architecture is unique and it is applicable to both microwave and millimeter wave systems such as 6G.

1. Introduction

In the last few years, a silent but quite dramatic, a revolution occurred in the development and production of autonomous electronic devices (e.g. laptops, smart phones, palm pilots, digital cameras, household robots, networked radios, base stations, etc.) that we use in our daily life. Currently, batteries power most of these devices and their disposal is environmental disaster. In future for energy transmission between two antennas repeater radios will be used [1] as shown in Figure 1, which are needed to be charged wireless because these radios will be deployed mostly in rural areas. This fact motivated us to think of solution that could enable wireless power transfer (WPT) using RF energy harvesting techniques to such devices.

Our WPT module is designed to charge a rechargeable battery (3 V and 1 mA) of a radio module. Existing techniques [2-5] (such as near-field inductive coupling, magnetic resonant coupling) for wireless power transfer allow transmission of tens of watts of power over a few meters. However, such techniques suffer from low efficiency and a smaller range. Here, we report the design of a WPT module using novel monolithic components on GaN at 5.8 GHz frequency (ISM band 4) that has potential to convert

**Corresponding Author:*
Rajinikanth Yella,
Electrical Engineering Computer Science (EECS), NCTU, Taiwan, China;
Email: rajini.02g@g2.nctu.edu.tw

 DOI: https://doi.org/10.30564/jeisr.v3i1.3549

the power efficiently and transfer the power to devices deployed in remote areas. Our research goal and its implementation are to maximize the distance of power transfer and to achieve maximum conversion efficiency.

An overview of the architecture and components for our proposed WPT module on a GaN chip is shown in Figure 1. The Integrated Chip (Figure 1) consist of various individual components such as; (i) Beamforming Antenna; (ii), Solar power feed to antenna; (iii) Photonic Power Converters, (iv) Filter; (v) Input matching circuits (vi) Rectifier, diode sensor (vi) and digital control circuit.

This paper only deals with the optimum design of individual components. It can be observed that sunlight striking on solar panel gives DC energy signal which is converted to photonic signal by PPC. The antenna acts as a transducer between PPC to decrease losses. A low pass filter will allow the signal to pass with a frequency lower than 5.8 GHz. It will then be converted to RF power signal by using rectifier. The sensor is used to check the correct device bias voltage and impedance of the rectifier.

Figure 2 shows proposed basic building blocks of the on-chip GaN WPT module. In the future, we will extend our proposed technologies to millimeter (mm) wave frequency, as there are several motivations to use mm-wave frequencies in radio links such as availability of wider bandwidth, relatively narrow beam widths, better spatial resolution and small wavelength allowing modest size antennas to have a small beam width.

The physical dimension of antennas becomes so compact that it good on practical to build complex antenna arrays integrate them on-chip. In this paper, we are presenting the design of the monolithic WPT module containing components from antenna to load as shown in Figure 2 is presented. The goal is to ultimately fabricate the monolithic WPT on GaN substrate

2. Photonics Power Converter (PPC)

In order to reduce losses in the WPT module, for remote device application a number of modules connected together of photonic power converter (PPC) can be used

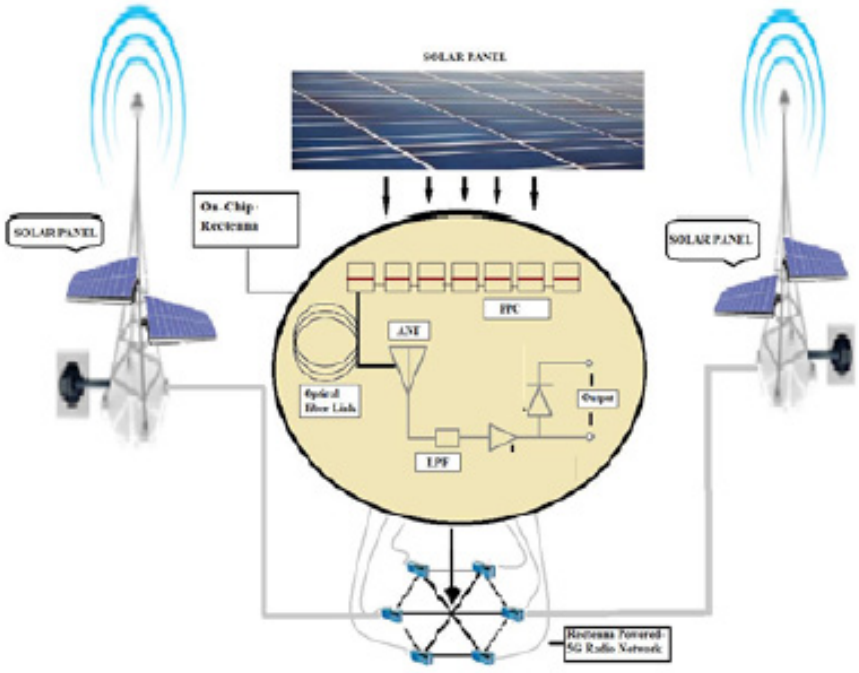

Figure 1. Proposed technology of WPT for 5G Network Communication

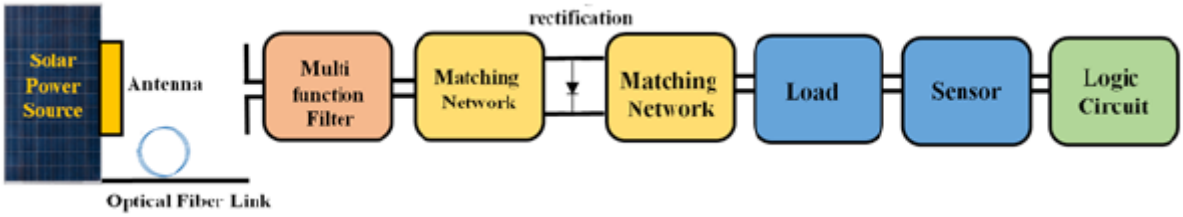

Figure 2. Proposed basic building blocks of WPT on same GaN chip

DOI: https://doi.org/10.30564/jeisr.v3i1.3549

for converting DC power to photonic into Electrical power, although PPCs are not required. So far for the photonic converters GaAs and Si materials have been used with optimization for absorption a different wavelength. For high conversion efficiencies GaAs has demonstrated 5. However, GaN is more suitable for PPC as it has wide bandgap, large breakdown voltage, and high electron saturation velocity. As shown in Figure 1, power from Solar cells will be launched into a photonic power converter (PPC) which will be a less than 2x2 mm GaN chip. To add voltages from the junctions several HEMT diodes connected in series, the amount of delivered current is proportional to the level of light power from solar cells illuminating the chip. PPC can be coupled with 980 nm fiber to transform the DC signal and finally expect to convert optical to electrical power. Our proposed idea, GaN photonic converter is expected to generate greater than 5 volts using a monolithic device chain. We expect optical-to-electrical power efficiency greater than 90% for the GaN PPC chip.

3. Antenna Design

Traditionally, antennas are off-chip due to their size and because typical substrates are conductive. However, if the antenna can be realized on-chip, it can result in a fully integrated system at a low cost. Monolithic Si-based integrated antennas have been demonstrated in recent years. However, standard silicon substrate is loss due to its low substrate resistivity, typically less than 100 cm. Moreover, the high dielectric constant of silicon causes most of the power to be absorbed in the substrate. This is a major drawback for antenna implementation on-chip, as it does not allow the energy to radiate efficiently into free space.

The mm-wave communication is widely accepted as a promising candidate for fifth and sixth generation (5G/6G) mobile communication systems 6 in order to handle massive data demand. According to the Friis transmission equation 7, by increasing the operation frequency, the signal wavelength becomes shorter and the path loss increases. Hence, in order to get the required gain overcoming attenuation effects, physically smaller antennas arranged as an array are desired.

In this paper, we are proposing two different kinds of on-chip GaN antennas for improvement in the radiation efficiency and gain using novel element design, the first one is beamforming array antenna (BFAA) and second one is multiple port wideband antenna (MPWBA). The true advantage of on-chip antenna can be attained by its realization in GaN chip process so that the circuits can be integrated with the back end digital blocks on the same chip because GaN will provide low loss, wide bandwidth, favorable linear polarization, and temperature stability [8-10].

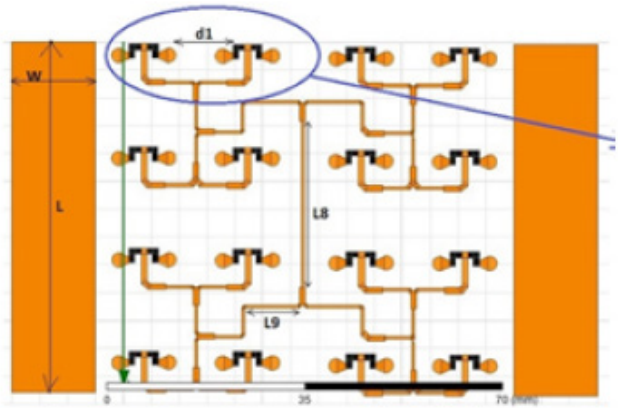

(a)

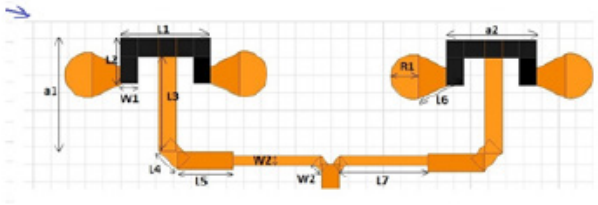

(b)

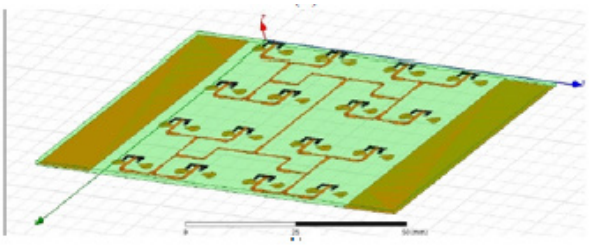

(c)

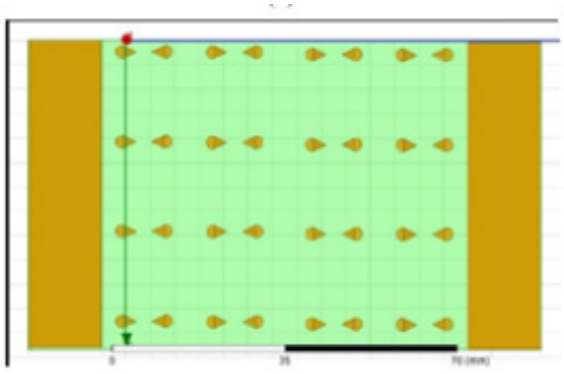

(d)

Figure 3. (a) Geometry of the proposed 4 X 4 antenna elements (b) single element (c) top view (d) bottom view

4. Beamforming Array Antenna (BFAA)

Generally, antenna arrays are used to generate a high gain. The antenna gain is proportional to its effective area.

DOI: https://doi.org/10.30564/jeisr.v3i1.3549

The higher antenna gain corresponds to the larger effective area and receives more electromagnetic power. One of the important parameters of array design, which must be accommodated very carefully, is set-out of the distance between the adjacent elements of an array. The decrement and increment in distance cause interference and distortion, not allowing further assessment of received signals [11]. Many mutual coupling reduction techniques have been proposed to improve the isolation performance between the antenna elements, such as neutralization line technology [12], electromagnetic bandgap [13-17], mush-room like decoupling structures [16] and meta-material decoupling [18,17,20]. By using these decoupling structures, isolation can be improved.

In this paper, we are proposing a two-layer beamforming a 4x4 array antenna with high isolation between elements. We have used high-frequency structure simulator (HFSS), full-wave solver, to design the antenna. The top layer is a T shape structure and bottom layer consists of drum type elements as shown in Figure 3a. For beamforming array, the distance between antenna elements is kept close to λ /4. Line length is adjusted to create delay between adjacent elements for beamforming radiation patterns. Dimensions of proposed antenna are mentioned in Table 1 (all dimensions in the Table 1 are in mm). The orange color in Figure 3a is gold material, yellow color is GaN material and light green color is GaN substrate.

Table 1. Dimensions of the proposed antenna

L	63	L5	3.2	W	15	a1	6.3
L1	5.2	L6	6.2	W1	1	a2	11.5
L2	2.5	L7	7.5	W2	0.5		
L3	5.3	L8	8.3	R1	1.5		
L4	1.5	L9	9.1	D1	7		

The configuration of our designed antenna array is shown in Figure 3. The antenna is comprised of T shaped with butterfly/drum-shaped patch elements. GaN was used as substrate while simulating antenna array. The substrate details which we used while simulating are, thickness of substrate is 1 mm, loss tangent value is 0 and relative permittivity is 9.7. The top layer is a T-shaped stub structure that is embedded in the GaN substrate, which has a distance of 0.1mm to the top surface of the substrate. The bottom layer is comprised of two inverted drum-shaped patches, which is embedded in the GaN substrate with a distance of 1 mm to the bottom of the GaN substrate.

The Figure 4 depicts the S11 response of the proposed antenna. The simulated S11 graph has -10 dB return loss from 5.67- 5.93 GHz, which means bandwidth of antenna is nearly 0.26 GHz. To overcome the performance degradation caused by beamforming usually we have to maintain mutual coupling between elements. In this paper we have maintained -30 dB.

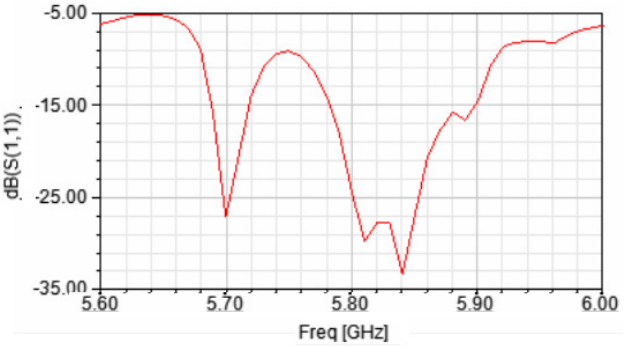

Figure 4. Return loss (S11) of BFAA

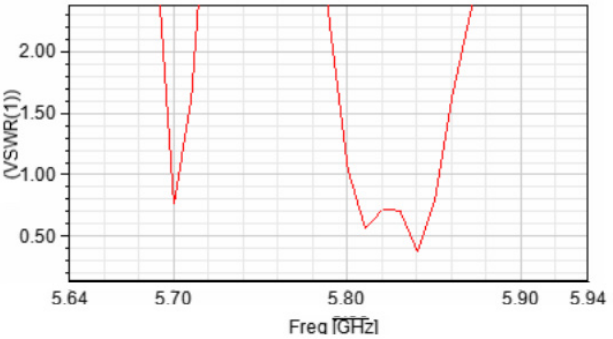

Figure 5. VSWR of BFAA

The Figure 5 shows VSWR (voltage standing wave ratio) of the antenna, usually for a good antenna VSWR should be below 2. Our simulation shows that for the passband frequency, antennas VSWR is below 1.2 as in Figure 5.

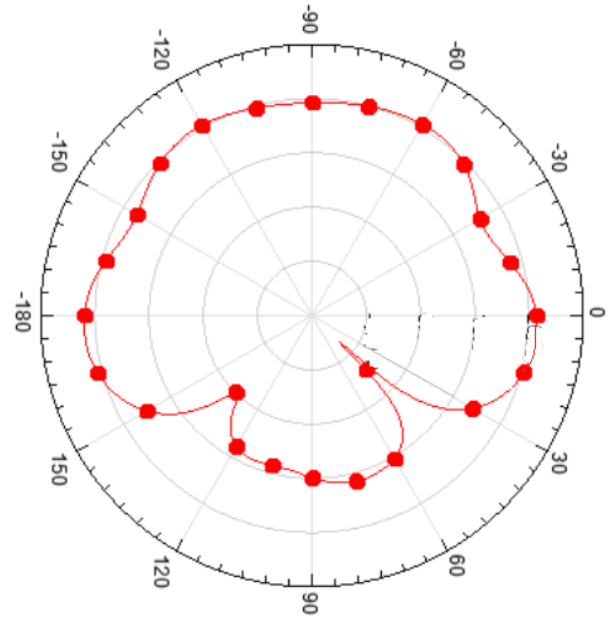

Figure 6. Radiation pattern of proposed antenna YZ plane

DOI: https://doi.org/10.30564/jeisr.v3i1.3549

The Figure 6 and Figure 7 are radiation patterns in YZ and XZ directions respectively. The patterns on the Smith chart indicate stability, low loss, and nearly ideal response.

The proposed BFAA 3D radiation pattern is shown in Figure 8. Our proposed antenna has maximum gain of 8.7 dB. From different angles, the proposed antenna has high gain, the overall antenna gain from 0° to 180° degree, ranges from 8.2 to 8.6 dB.

It is observed from the Figure 9 that the proposed antenna is maintaining good range current whole structure.

4.1 Design of Multiport Wide Band Antenna (MPWBA)

In our proposal, we also plan, alternately, to integrate multiport wideband antenna (MPWBA) on GaN chip for the

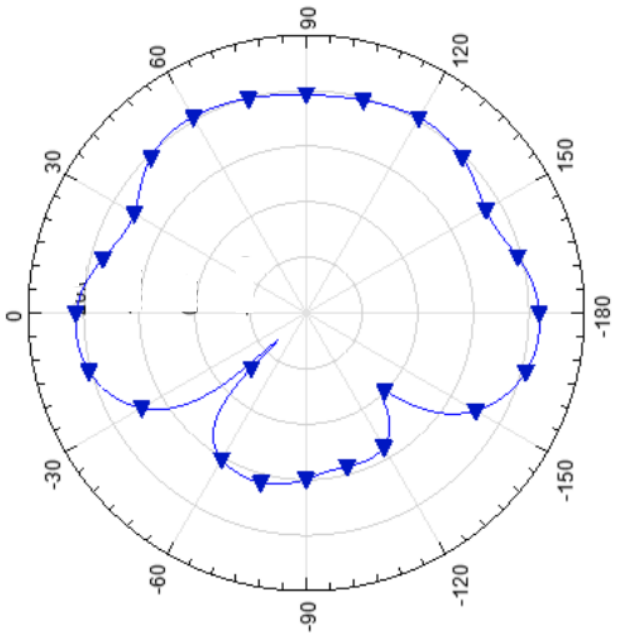

Figure 7. Radiation pattern of proposed antenna XZ plane

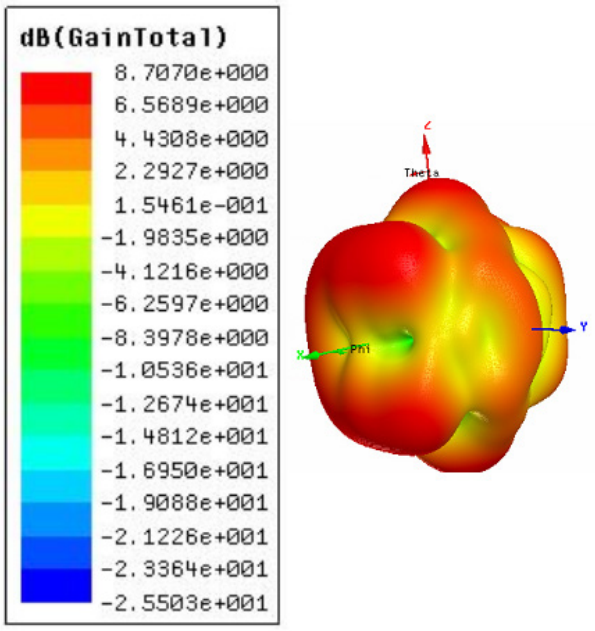

Figure 8. The 3D radiation pattern of proposed BFAA

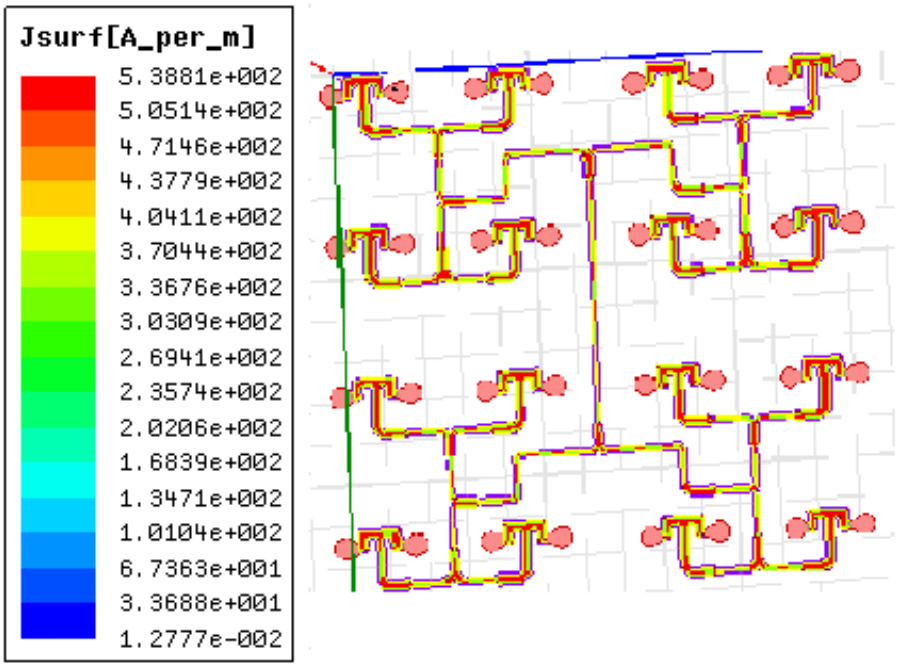

Figure 9. Current density distribution of BFAA

 DOI: https://doi.org/10.30564/jeisr.v3i1.3549

wideband spectrum. Wideband antennas with high efficiency are needed for both cellular access and backhaul networks 19 to cover a wide angular area with a single antenna. We have used HFSS full-wave solver to design the antenna. The dimensions of proposed antenna are mentioned in Table 2 (all dimensions in the Table 2 are in mm).

Table 2. Dimensions of proposed MPWBA

L	W	L1	L2	W1	W2
8	4	1	1	0.5	0.2

The configuration of our designed MPWBA is shown in Figure 10. The antenna is comprised of square shape, three C shaped structures are connected to four sides of square as shown in Figure 10, distance between two C shaped structures are maintained close to _/8. Left and right C shape structures are assumed as input ports. GaN was used as substrate while simulating antenna array. The substrate details which we used while simulating are, thickness of substrate is 1mm, loss tangent value is 0 and relative permittivity is 9.7. The top layer has MPWBA which is embedded in the GaN substrate, which has a distance of 0.1mm to the top surface of the substrate. The bottom layer is assumed as ground. The pink color in Figure 10 is gold material, green color is GaN material and light green color is GaN substrate. Our proposed MPWBA antenna can work with multiple ports, from port 1 to port 12. Our proposed antenna will give best performance with port 7.

The Figure 11 depicts the S11 response of the proposed MPWBA. The proposed MPWBA has return loss of -32 dB with input ports 1 & 2, -46 dB with port 7, and -15dB with remaining ports. The bandwidth of the antenna is

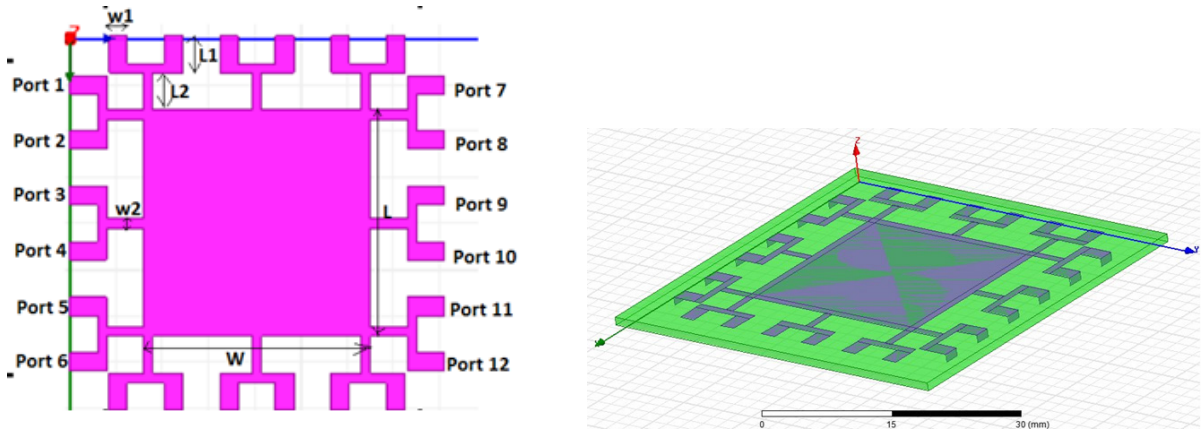

(a) (b)

Figure 10. (a) Geometry of the proposed MPWBA (b)3D top view of MPWBA

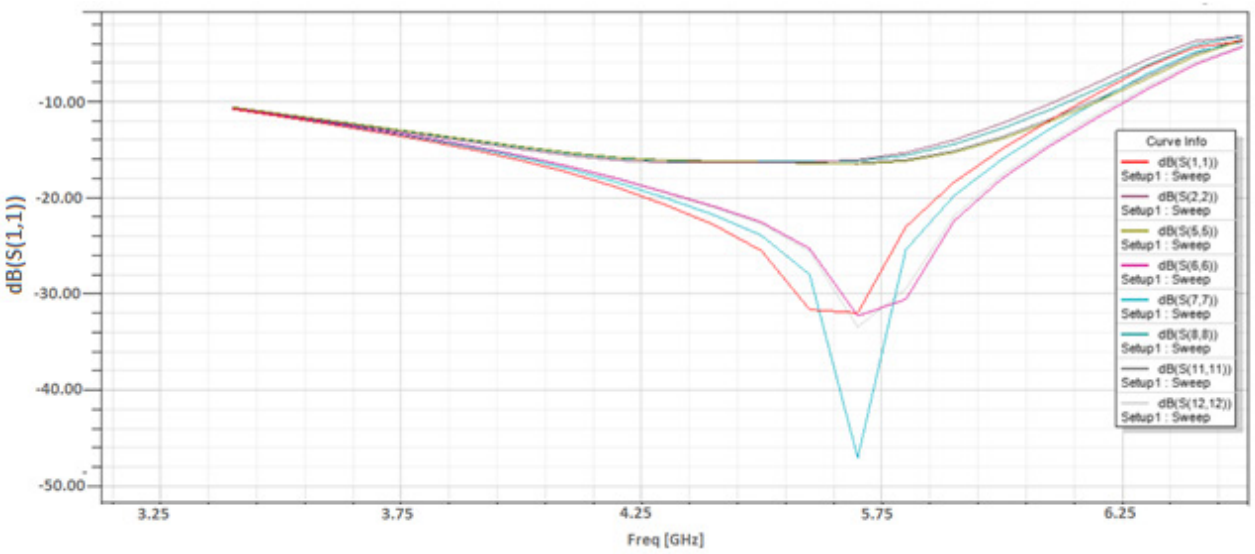

Figure 11. Return loss (S11) response of MPWBA

DOI: https://doi.org/10.30564/jeisr.v3i1.3549

nearly 3 GHz (3.5 GHz to 6.5 GHz).

The Figure 12 shows VSWR (voltage standing wave ratio) of MPWBA, which is nearly 0.75 which is enough for rejecting unwanted signals and to satisfy the bandwidth requirement for specified frequency range. The proposed MPWBA 3D radiation pattern is shown in Figure 13. Our proposed antenna has maximum gain of 7.3 dB. It indicates that very good polarization proposed antenna. The Figure 14a, b are radiation patterns in YZ and XZ directions respectively.

The simulated results of proposed BFAA and MPWBA are mentioned in the below Table 3.

Table 3. Performance comparison table of BFAA and MP-WBA

Content	units		
Antenna type		BFAA	MPWBA
Single antenna size (L*W)	mm*mm	6.3*11.5	8*12
Antenna array size (L*W)	mm*mm	63*67	
Return loss S11	dB	34	46
Antenna gain	dB	8.7	7.3
Peak Directivity	dB	8.9	5.6
Antenna bandwidth	GHz	5.67-5.93	3.5-6.5
Radiated power	dBm	23	20.7
Accepted power	dBm	25	22
Radiation Efficiency	%	93	87
VSWR	GHz	1.2	0.75

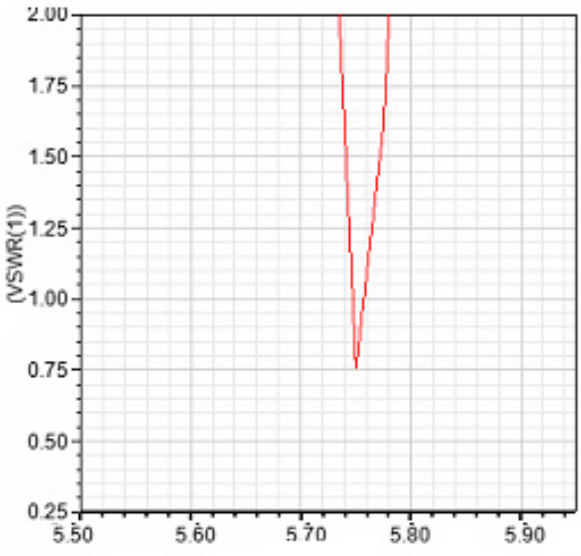

Figure 12. VSWR response of MPWBA

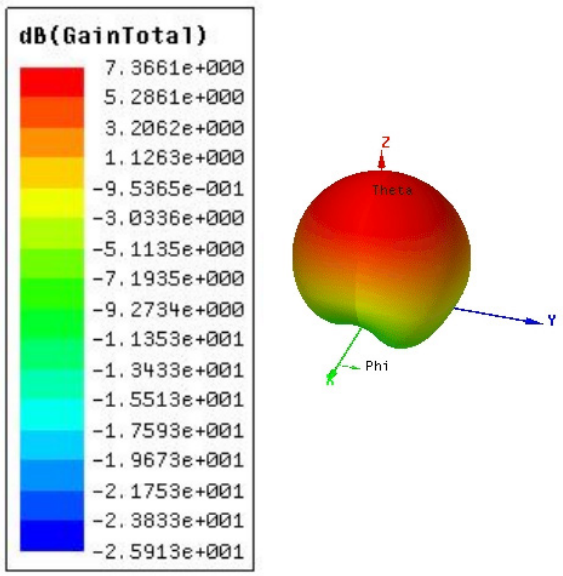

Figure 13. The 3D radiation pattern of proposed MPWBA from HFSS

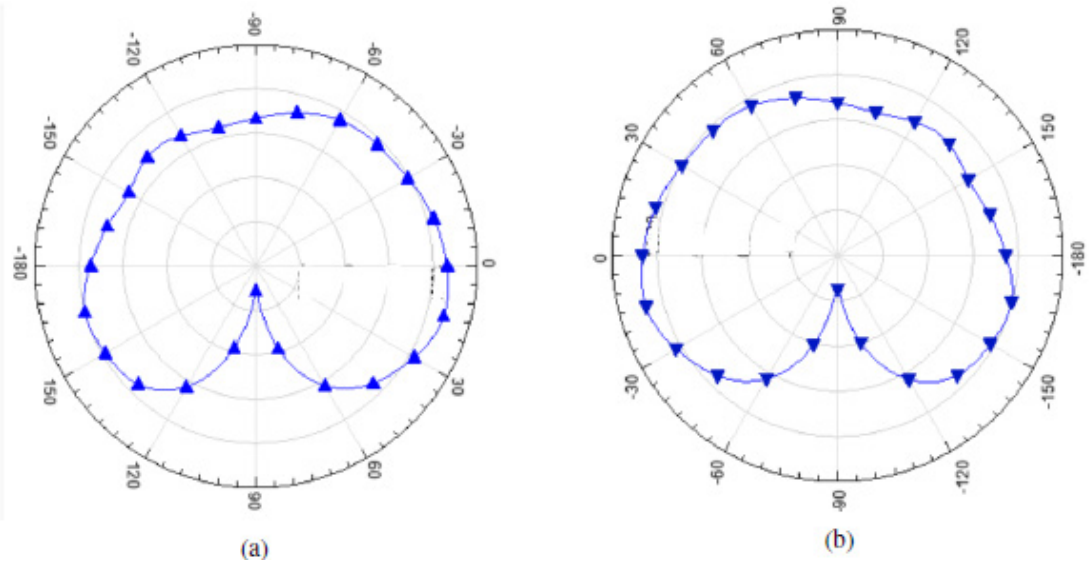

Figure 14. (a) Radiation pattern of proposed antenna in YZ plane (b) Radiation pattern of proposed antenna in XZ plane

 DOI: https://doi.org/10.30564/jeisr.v3i1.3549

5. Impedance Matching Network

In this paper, the power conversion process is proposed at 5.8 GHz frequency. At such frequency, the reflected power occurs when the load impedance is not matched to the characteristic impedance of source impedance. Traditionally spiral inductors are preferred instead of resistors and transmission lines to enhance the thermal noise performance; however, they cannot be used at high frequency because of the self-resonance and stray impedances. In addition, they also occupy a large onchip space. In order to overcome such problems, we adopted a new design strategy in this paper. The proposed approach is based on closed-form and recursive relationships [22]. We calculated stub values using ADS object function to optimize the whole matching networks. During 5.7 GHz to 5.9 GHz, the maximum transducer gain limit to 64dB and the minimum transducer gain is 63dB. As a result, we can get a good transducer curve, whose flatness is less than ±0.2 dB at desired frequency of 5. 8 GHz. Traditionally Network Response is calculated to check the loss value of circuit. So we plotted S11 to find the loss of the network schematic, the S11 value at 5.8 GHz is lower than -10 dB. To investigate circuit stability and perfect match we plotted impedance (Figure 15) on Smith chart as shown in Figure 15.

6. Design and Optimization of Multifunction Filter

As shown in Figure 19, we need two filters for the design of the rectifier circuit. One is at input side and one is at output side. In this paper, we are using our multifunction filter circuit 21. The core LPF circuit with minor changes is converted into BPF and HPF. For BPF a matching network is added at the output of LPF, addition of matching network does not contribute significant loss as evident from the value of S11.

6.1 Low Pass Filter (LPF)

In our proposed filter concept, the number of poles decides range of cut-off frequency of a filter. For example, we designed LPF circuit with cut-off frequency of 5.8 GHz, therefore, we placed 5 poles. To enhance attenuation in the stopband, length and width of the poles of proposed filter are adjusted. P1 and P5 are identical as well as P2 & P4 are identical in length and width. Length of P1 or P5 length of P2 or P4 length of P3. Whereas the Width of poles should be such that width of P3 width of P2 or P4 width of P1 or P5. For microstrip filters optimum distance between poles is also very crucial as this length will act as capacitive or inductive (depending upon the frequency

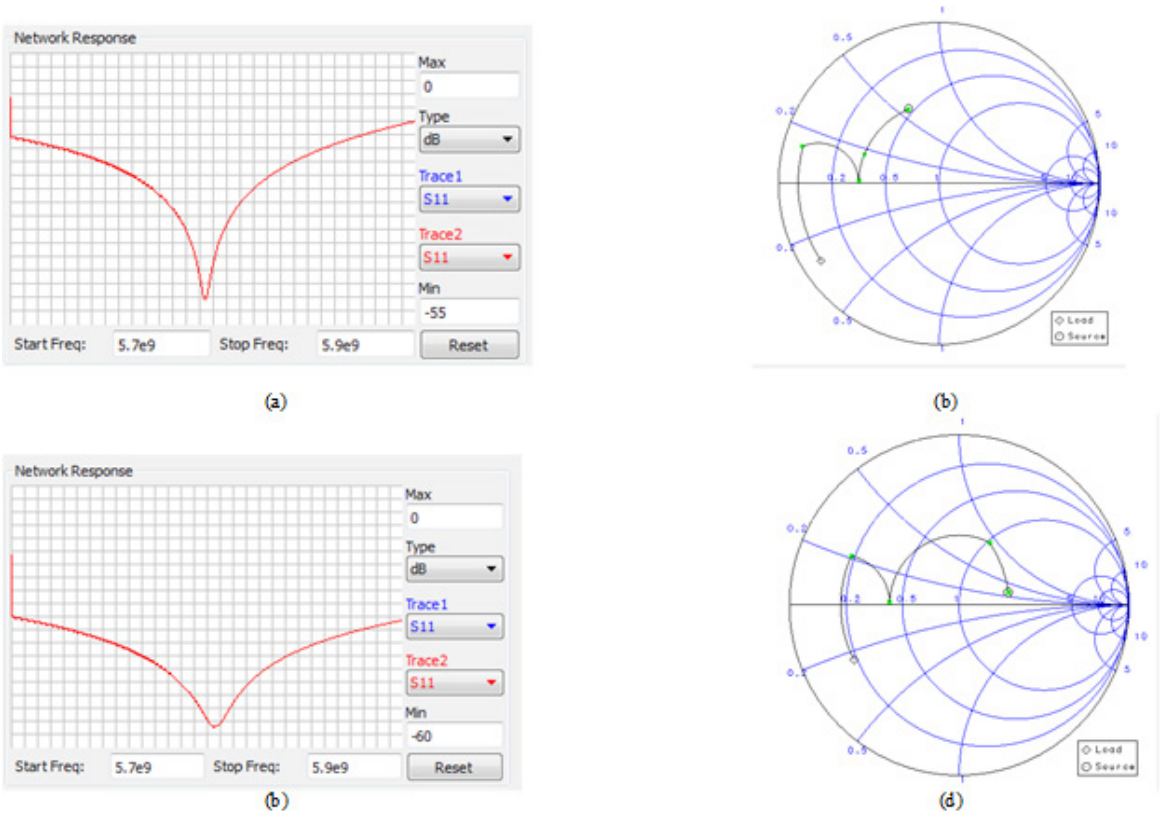

Figure 15. (a) Radiation pattern of proposed antenna in YZ plane (b) Radiation pattern of proposed antenna in XZ plane

DOI: https://doi.org/10.30564/jeisr.v3i1.3549

of operation and distance between poles). The passband frequency could be adjusted via the structure parameters of the poles. The designed multifunction filter is simple in structure and compact in size.

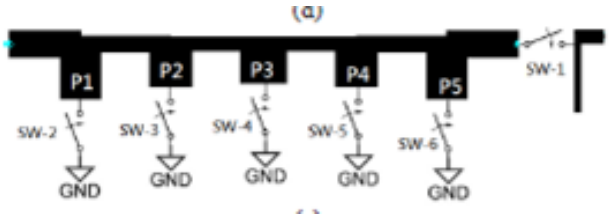

Figure 16. Multimode filter

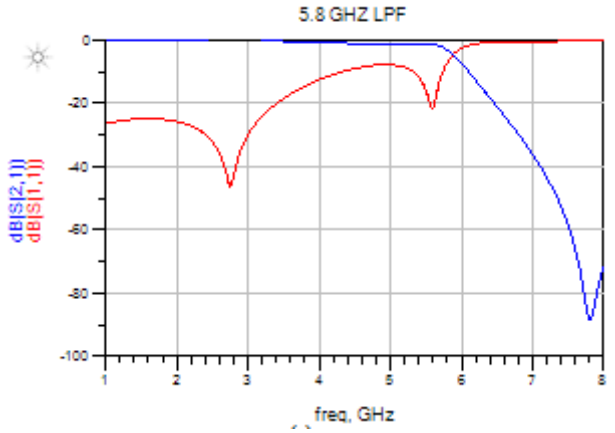

Figure 17. S11 and S21 response of LPF

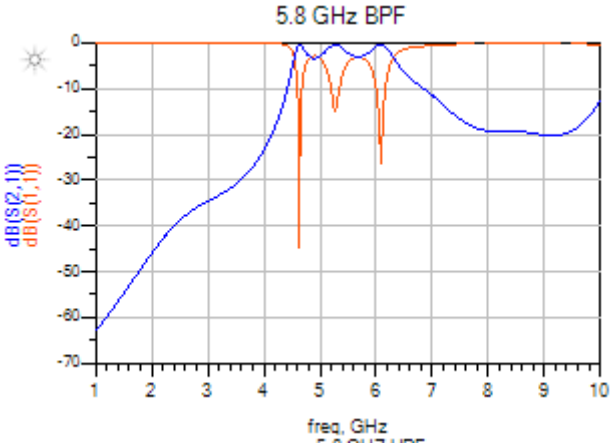

Figure 18. S11 and S21 response of BPF

Figure 17 depicts response of proposed LPF. In case of LPF, simulated -3 dB passband range is obtained from DC to 5.85 GHz. B. Band Pass Filter (BPF). As mentioned above, the LPF circuit with minor changes behaves like BPF. For BPF a matching network is added at the output of LPF. The addition of matching network does not contribute significant loss as evident from the value of S11 (lower than-20 dB). The BPF passband at the desired frequency is realized by adjusting the structure parameters of the matching network. Figure 18, presents simulated of proposed BPF.

7. Rectifier Design

We have used a PNP transistor as a diode while designing the rectifier circuit. Agilent ADS is used for rectifier design with the concept is, 1) To measure the S-parameter values of PNP diode. 2) Design the rectifier circuit according to the Figure 19 by de-embedding the S-parameter values. 3) We have to make sure that the input RF signal should be supplied to rectifier circuit without any significant loss. To achieve this, we have activated LPF from the multifunction filter block using switch1 as shown in Figure 16. 4) Design input matching network between LPF and rectifier. 5) Harmonics are generated during the RF to DC conversion process, which should be removed before collecting the DC power. BPF (is activated from the multifunction filter) is added at rectifier output side to remove unwanted harmonics. Figure 22b shows that even harmonics of rectifiers are attenuated (¡-50dB) at 5.8 GHz frequency with BPF. 6)Optimize the impedance matching network of BPF circuit so that rectifier should give high efficiency with low load resistance values without compromising attenuation of harmonics. 7)Design output matching network between BPF and load.

To investigate the loss of proposed WPT architecture, we have simulated S11 of WPT module chain with BFAA and MPWBA in ADS. The results are shown in Figure 20.

Traditionally S11 is calculated to check the return loss value of circuit. So we plotted S11 to find the loss of the whole architecture (antenna, filter, input matching network, rectifier, output matching network and load) the S11 value at 5.8 GHz is lower than -10dB. Figure 20 indicates that input and matching networks, input and output filter networks are worked well along with the design concepts. Our proposed design has achieved the return loss of about -31.9 dB, -27.8 dB, at 5.8 GHz for BFAA and MPWBA respectively.

To check the performance of rectifier power conversion efficiency (PCE) is an important factor, which denotes how efficiently the rectifier converts the input RF power to DC power. Harmonic balance (HB) simulation is used in ADS to calculate PCE. PCE can be calculated by using

$$PCE = \frac{P_{out}}{P_{RFpower}} * 100 \quad (1)$$

$$P_{out} = \frac{V_{DC}^2}{R_{LOAD}} \quad (2)$$

Figure 21 shows the PCE performance graphs of pro-

DOI: https://doi.org/10.30564/jeisr.v3i1.3549

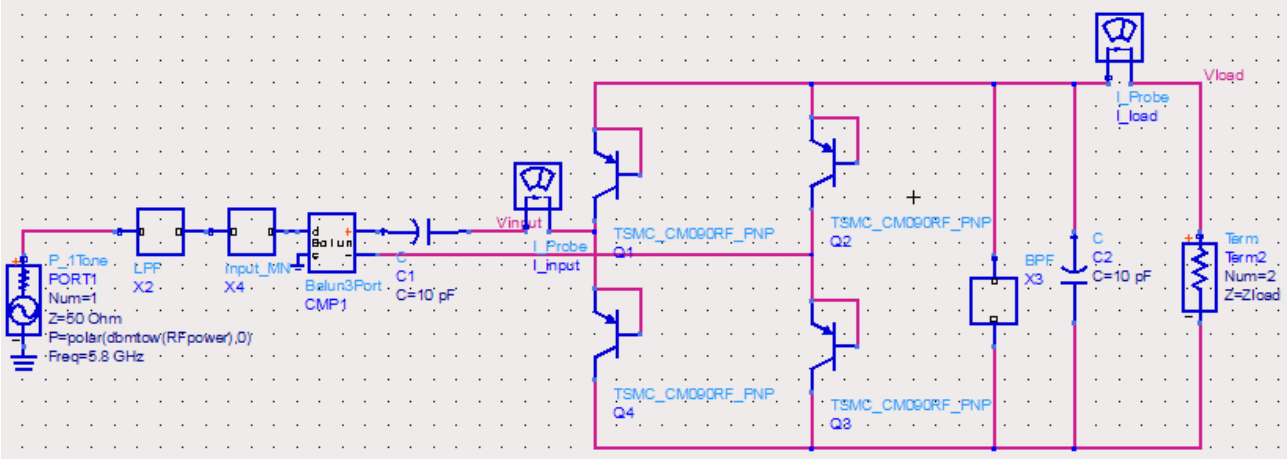

Figure 19. Schematic diagram of proposed rectifier

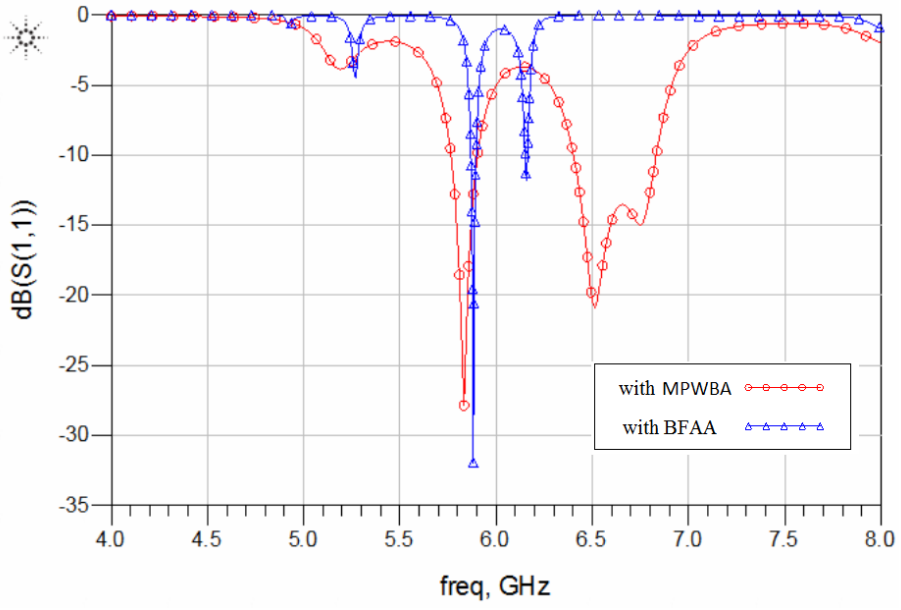

Figure 20. Return loss (S11) of WPT module chain with BFAA and MPWBA

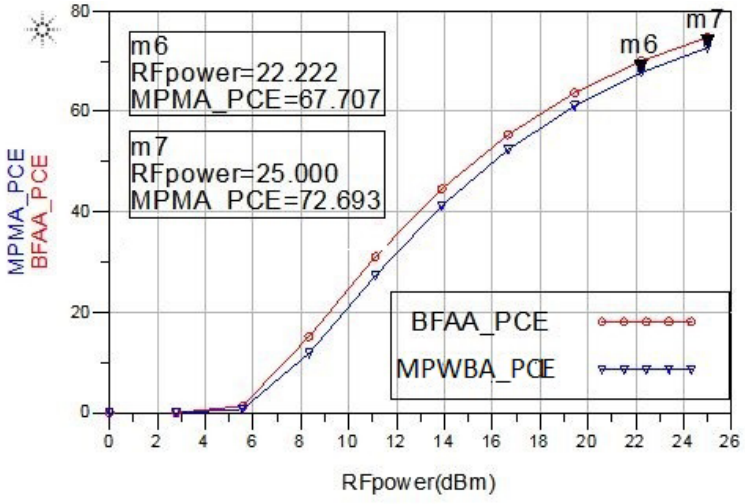

Figure 21. PCE of the proposed rectifier with BFAA and MPWBA

DOI: https://doi.org/10.30564/jeisr.v3i1.3549

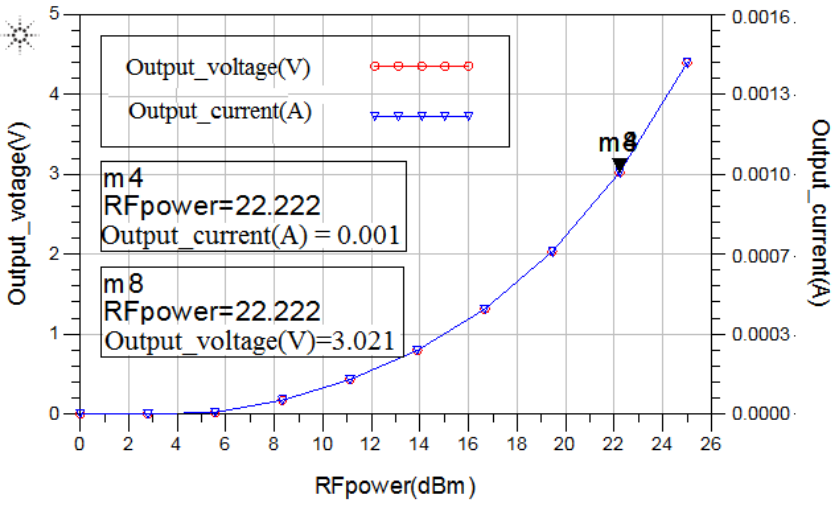

Figure 22. (a) Output voltage graph of rectifier (b) Harmonics of rectifier at 5.8 GHz frequency

Table 4. Design specification comparison of proposed work with previously published works

		[26]	[27]	[28]	[29]	[30]	[31]	[32]	My work	
Year		2005	2010	2011	2013	2015	2016	2017	2021	2021
Frequency	GHz	5.8	2.45	2.45	5.8	5.8	16.5	245	5.8	5.8
Output Voltage	V	3.41	3.64	2.82	0.18	1.41	1.2	5	3	3
Output Current	mA	12	3.46	0.18	0.4	14	-	10	1	1
Conversion Efficiecny	%	68.5	52	63	37	64.8	63	5.5	67	74
Load	Ω	270	1050	50	1000	100	10000	500	80	40

posed rectifiers. The PCE for rectifier with BFA antenna and MPM antenna is 72% and 67%, with an optimal load resistance 40 ohm and 80 ohms respectively. Our rectifier circuit is designed to charge a 5G/6G radio module rechargeable battery of 3 V, 1 mA.

The simulated output DC voltage and current against the input power are shown in Figure 22a. A comparison of performances of proposed work with previously published works from 2005 to 2017 is highlighted in Table 4. Power conversion efficiency is better than previously published papers.

8. Conclusions

The design of a novel WPT module using monolithic components on the GaN substrate is presented in this paper. The WPT module consists of BFAA, PPC, LPF, input matching network, rectifier, and output matching network. logic circuit can be designed and built on substrate or keep it off-chip. We investigated innovative designs for the WPT components with potential for integration on a GaN substrate. Monolithic WPT module shows loss of less than -10 dB at 5.8 GHz which can be further improved with design refinement. To validate our designs, we selected 5.8 GHz ISM band but module design can be easily scaled to millimeter-wave frequencies such as 28 GHz being considered for 5G/6G system. To our knowledge, this first reported design of WPT module on GaN chip. Our proposed module will offer significant SWAP-C advantages. Our proposed rectifier has RF-DC conversion efficiency of 74% and 67% with beam-forming antenna and multiple port antenna respectively. Our WPT module is designed to charge a rechargeable battery (3 V and 1 mA) of a radio module which will be used between two antennas in future 5G/6G networks. In the future, we will extend our proposed technologies to millimeter (mm) wave frequency, as there are several motivations to use mm-wave frequencies in radio links such as availability of wider bandwidth, relatively narrow beam widths, better spatial resolution and small wavelength allowing modest size antennas to have a small beam width.

 DOI: https://doi.org/10.30564/jeisr.v3i1.3549

Acknowledgments

We are thankful to our National Chiao Tung University, Taiwan for providing the facilities to carry out our research.

References

[1] Advanced Antenna Systems for 5G," America, Tech. Rep., 2019.

[2] S. Y. Choi, B. W. Gu, S. W. Lee, W. Y. Lee, J. Huh, and C. T.Rim, "Generalized Active EMF Cancel Methods for Wireless Electric Vehicles," IEEE Transaction on Power Electronics, vol. 29, no. 11, pp.5770-5783, Nov 2014.

[3] S. Y. R. Hui, W. Zhong, and C. K. Lee, "A Critical Review of Recent Progress in Mid-Range Wireless Power Transfer," IEEE Transactions on Power Electronics, vol. 29, no. 9, pp. 4500-4511, Sep 2014.

[4] C. A. Tucker, U. Muehlmann, and M. Gebhart, "Contactless power transmission for NFC antennas in credit-card size format," IET Circuits, Devices and Systems, vol. 11, no. 1, pp. 95-101, 2017.

[5] J. Chu, W. Gu, W. Niu, and A. Shen, "Frequency splitting patterns in wireless power relay transfer," IET Circuits, Devices Systems, vol. 8, no. 6, pp. 561-567, Nov 2014.

[6] W. X. Zhong, C. Zhang, X. Liu, and S. Y. R. Hui, "A Methodology for Making a Three-Coil Wireless Power Transfer System More Energy Efficient Than a Two-Coil Counterpart for Extended Transfer Distance," IEEE Transactions on Power Electronics, vol. 30, no. 2, pp. 933-942, Feb 2015.

[7] J. B. Rosolem, "Powerˆa A ROverˆa€A RFiber Applications for Telecommunications and for Electric Utilities," in Optical Fiber and Wireless Communications. InTech, June 2017.

[8] J. Zhang, X. Ge, Q. Li, M. Guizani, and Y. Zhang, "5G Millimeter-Wave Antenna Array: Design and Challenges," IEEE Wireless Communications, vol. 24, no. 2, pp. 106-112, Apr 2017.

[9] Rajinikanth Yella, Krishna Pande, Ke Horng Chen, Edward Chang 28 GHz Monolithic Transmitter on GaN chip for 5G application. The Tenth International Conference on Advances in Satellite and Space Communications SPACOMM 2018.

[10] Rajinikanth Yella, Krishna Pande, Ke Horng Chen, Edward Chang Design of On-Chip GaN transmitter for wireless communication, International Journal On Advances in Telecommunications 2018.

[11] T. S. Rappaport, Shu Sun, R. Mayzus, Hang Zhao, Y. Azar, K. Wang, G. N. Wong, J. K. Schulz, M. Samimi, and F. Gutierrez, "Millimeter Wave Mobile Communications for 5G Cellular: It Will Work!" IEEE Access, vol. 1, pp. 335-349, 2013.

[12] Q. Luo, S. Gao, N. Carvalho, K. Osipov, J. Wurfl, R. Vilaseca, D. Pham-Minh, A. Marques, J. Pinto, and R. Martins, "GaN-Integrated Beam-Switching High-Power Active Array for Satellite Communications," in 12th European Conference on Antennas and Propagation (EuCAP 2018). Institution of Engineering and Technology, 2018, pp. 621 (5 pp.)-621 (5 pp.).

[13] D. Liu, B. Gaucher, U. Pfeiffer, and J. Grzyb, Eds., Advanced Millimeter-Wave Technologies. Chichester, UK: John Wiley Sons, Ltd, feb 2009.

[14] C. Narayan, Antennas And Propagation. Technical Publications, 2007.

[15] S. Zhang and G. F. Pedersen, "Mutual Coupling Reduction for UWB MIMO Antennas With a Wideband Neutralization Line," IEEE Antennas and Wireless Propagation Letters, vol. 15, pp. 166-169, 2016.

[16] J.-Y. Lee, S.-H. Kim, and J.-H. Jang, "Reduction of Mutual Coupling in Planar Multiple Antenna by Using 1-D EBG and SRR Structures," IEEE Transactions on Antennas and Propagation, vol. 63, no. 9, pp. 4194-4198, Sep 2015.

[17] Q. Li, A. P. Feresidis, M. Mavridou, and P. S. Hall, "Miniaturized Double-Layer EBG Structures for Broadband Mutual Coupling Reduction Between UWB Monopoles," IEEE Transactions on Antennas and Propagation, vol. 63, no. 3, pp. 1168-1171, Mar 2015.

[18] T. Jiang, T. Jiao, and Y. Li, "Array Mutual Coupling Reduction Using LLoading E-Shaped Electromagnetic Band Gap Structures," International Journal of Antennas and Propagation, vol. 2016, pp. 1-9, 2016.

[19] Fan Yang and Y. Rahmat-Samii, "Microstrip antennas integrated with electromagnetic band-gap (EBG) structures: A low mutual coupling design for array applications," IEEE Transactions on Antennas and Propagation, vol. 51, no. 10, pp. 2936-2946, Oct 2003.

[20] W. Liu, Z. N. Chen, and X. Qing, "Metamaterial-Based Low-Profile Broadband Mushroom Antenna," IEEE Transactions on Antennas and Propagation, vol. 62, no. 3, pp. 1165-1172, Mar 2014.

[21] R. HafeziFard, M. Naser-Moghadasi, J. Rashed-Mohassel, and R.-A. Sadeghzadeh Sheikhan, "Mutual Coupling Reduction for Two Closely- Space Meander Line Antennas Using Metamaterial Substrate," IEEE Antennas and Wireless Propagation Letters, vol. 15, pp. 1-1, 2015.

DOI: https://doi.org/10.30564/jeisr.v3i1.3549

[22] Xin Mi Yang, Xue Guan Liu, Xiao Yang Zhou, and Tie Jun Cui, "Reduction of Mutual Coupling Between Closely Packed Patch Antennas Using Waveguided Metamaterials," IEEE Antennas and Wireless Propagation Letters, vol. 11, pp. 389-391, 2012.

[23] P. Simon, "Analysis and Synthesis of Rotman Lenses," in 22nd AIAA International Communications Satellite Systems Conference Exhibit 2004 (ICSSC), no. May. Reston, Virginia: American Institute of Aeronautics and Astronautics, May 2004, pp. 1-11.

[24] E. C. Rajinikanth Yella, Krishna Pande, and Ke Horng Chen, "Design of On-Chip GaN Transmitter for Wireless Communication," International Journal on Advances in Telecommunications, vol. 11, pp. 125-133, 2018.

[25] R. Yella, K. Pande, K. H. Chen, and L.-C. Wang, "Design and Fabrication of Stepped Impedance Multi-Function Filter," International Journal of Electrical and Computer Systems, vol. 4, pp. 1-5, 2018.

[26] C.-H. Chin, Quan Xue, and Chi Hou Chan, "Design of a 5.8-GHz rectenna incorporating a new patch antenna," IEEE Antennas and.

[27] Wireless Propagation Letters, vol. 4, no. 1, pp. 175-178, 2005.

[28] H. Takhedmit, B. Merabet, L. Cirio, B. Allard, F. Costa, C. Vollaire, and O. Picon,"A 2.45-GHz low cost and efficient rectenna," in EuCAP 2010 - The 4th European Conference on Antennas and Propagation. IEEE, 2010, pp. 1-5.

[29] Z. Harouni, L. Cirio, L. Osman, A. Gharsallah, and O. Picon, "A Dual Circularly Polarized 2.45-GHz Rectenna for Wireless Power Transmission," IEEE Antennas and Wireless Propagation Letters, vol. 10, pp. 306-309, 2011.

[30] T. Matsunaga, E. Nishiyama, and I. Toyoda, "5.8-GHz stacked differential mode rectenna suitable for large-scale rectenna arrays," in 2013 Asia-Pacific Microwave Conference Proceedings (APMC). IEEE, Nov 2013, pp. 1200-1202.

[31] P. Lu, X.-S. Yang, J.-L. Li, and B.-Z. Wang, "A Compact Frequency Reconfigurable Rectenna for 5.2- and 5.8-GHz Wireless Power Transmission," IEEE Transactions on Power Electronics, vol. 30, no. 11, pp. 6006-6010, Nov 2015.

[32] C. Wang, K. Zhao, Q. Guo, and Z. Li, "Efficient self-powered convertor with digitally controlled oscillator-based adaptive maximum power point tracking and RF kick-start for ultralow-voltage thermoelectric energy harvesting," IET Circuits, Devices Systems, vol. 10, no. 2, pp. 147-155, Mar 2016.

[33] P. Kundu (Datta), J. Acharjee, and K. Mandal, "Design of an Efficient Rectifier Circuit for RF Energy Harvesting System," international journal of advanced engineering and management, vol. 2, no. 4, p. 94, Apr 2017.

 DOI: https://doi.org/10.30564/jeisr.v3i1.3549

BILINGUAL PUBLISHING CO.
Pioneer of Global Academics Since 1984

Journal of Electronic & Information Systems
https://ojs.bilpublishing.com/index.php/jeis

ARTICLE

Circular Ribbon Antenna Array Design For Imaging Application

Rajinikanth Yella[1*] Krishna Pande[2] Ke Horng Chen[2]

1. Electrical Engineering Computer Science (EECS), NCTU, Taiwan, China
2. Electrical Engineering (EE), NCTU, Taiwan, China

ARTICLE INFO

Article history
Received: 11 August 2021
Accepted: 20 August 2021
Published Online: 30 August 2021

Keywords:
Beamforming antenna
Antenna array
Advanced design system (ADS)
Biomedical imaging

ABSTRACT

Our goal is to develop THz module on chip to visualize bone grinding at the early stage so that arthritis can be visualized and treated early. A critical component of such module is antenna. A compact 4 by 4 beamforming antenna array for biomedical application is presented in this paper. We are proposing a novel antenna which is in the form of a circular ribbon shape with a gold patch. Gold material for the patch is used to enhance its conductivity and to cut down backward radiation. Differential port pin used to increase the bandwidth. Au-posts are finally used for output connection. The proposed antenna operates over the frequency band from 201 GHz to more than 228 GHz. Directivity and gain of the proposed antenna are 13 dB and 7 dB respectively. This makes it applicable for imaging systems because of the frequency band for biomedical imaging. Index Terms—Beamforming antenna, antenna array, Advanced design system (ADS), Biomedical imaging.

1. Introduction

THz communications are one of the possibilities to meet the demand for ever-increasing data rates. In recent years, several publications have reported a 100 -300 GHz antenna design with a target for enhanced biomedical applications [1,2]. Microwave imaging from 100 to 300 GHz is an auspicious design for biomedical applications such as detecting the skin cancer. Reason is that it has good resolution and generation characteristics [3]. The process for skin cancer detection with the high-frequency module on chip containing antenna is initially a pulse that is transmitted from the antenna, which will penetrate through the various tissues of the body. At a particular time, the transmitted signal will be reflected from the small size. Particles which represent that skin cancer.

The same antenna can be used to collect the reflected signal for further measurements. For accurate results, the antenna should have high gain, directivity, resolution, dynamic range with compact size [4]. Also such technology is beneficial for the detection of Arthritic. Many antenna designs have been proposed for biomedical imaging applications [5,6], each has its advantages and drawbacks. Some published antennas have a structure of rectangular ribbon type, whereas others have a square structure. All the proposed structures are using only a single antenna for detecting the signal. As a result, weaker signals go undetected. In this paper, we are proposing a compact size 2.8*0.43 mm^2 circular ribbon-shaped beamforming identify applicable funding agency here. If none, delete this antenna array with high gain and directivity. In addition, we are also studying application of meta material elements for this application.

**Corresponding Author:*
Rajinikanth Yella,
Electrical Engineering Computer Science (EECS), NCTU, Taiwan, China;
Email: rajini.02g@g2.nctu.edu.tw

DOI: https://doi.org/10.30564/jeisr.v3i1.3550

2. Design Methodology

Traditionally, antennas are off-chip due to their size and because typical substrates are conductive [7,8]. The proposed circularly ribbon-shaped antenna is shown in Figure 1. To enhance its conductivity and to cut down backward radiation gold material was used for the patch. Differential port pin used to increase the bandwidth. Dimensions of the antenna are angle radius of the circle is 100 um with a thickness of 10 um and patch length 100 um with a thickness of 10 um.

Generally, antenna arrays are used to generate a high gain. One of the important parameters of array design is the setout of the distance between the adjacent elements of an array because this will lead to interference and distortion, not allowing further assessment of received signals [9]. Many mutual coupling contraction techniques [10-12] have been proposed to enhance the isolation performance between the antenna elements.

In this paper I am proposing a two-layer beamforming a 4x4 array antenna with high isolation between elements. I have used ADS to design the antenna. The top layer is a circular shape structure. For beamforming array, the distance between antenna elements is kept close to /4. Line length is adjusted to create a delay between adjacent elements for beamforming radiation patterns. GaN was used as a substrate while simulating antenna array. The configuration of our designed antenna array is shown in Figure 2.

3. Results

The Figure 3 depicts the S11 response of the proposed antenna. The simulated S11 graph has -10 dB return loss from 201.6GHz to 228.1 GHz, which means the bandwidth of the antenna is nearly 26.5 GHz. Peak S11 is noticed at 217.2 GHz with a value of -41.9 dB.

The Figure 4 shows gain and directivity plot of the proposed antenna has 7 dB gain and 13 dB directivity at 217 GHz frequency. The proposed antenna has maximum gain and directivity at 250 GHz frequency.

The Figure 5 and Figure 6 depict 3D radiation patterns in YZ and XZ directions respectively. The simulated results of the proposed antenna are mentioned in the Table 1.

Table 1. proposed antenna results

content	units	
Single antenna size (L*W)	um*um	500*615
Antenna array size (L*W)	um*um	2.8*0.43
Return Loss (S11)	dB	-41.8
Antenna Gain	dB	7
Directivity	dB	13
Antenna Bandwidth	GHz	28.5

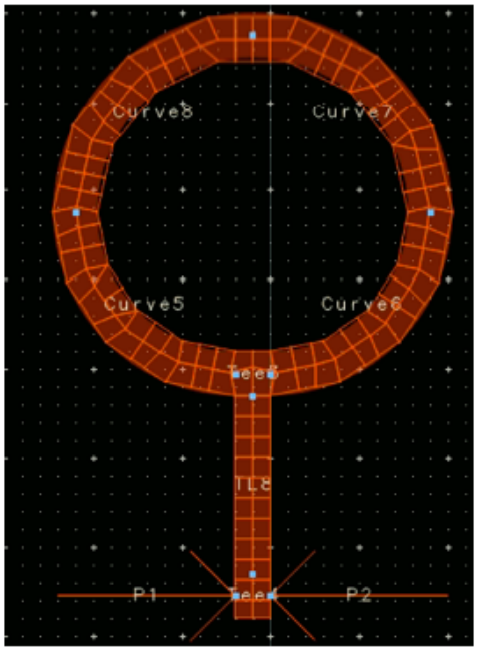

Figure 1. Proposed circular ribbon-shaped

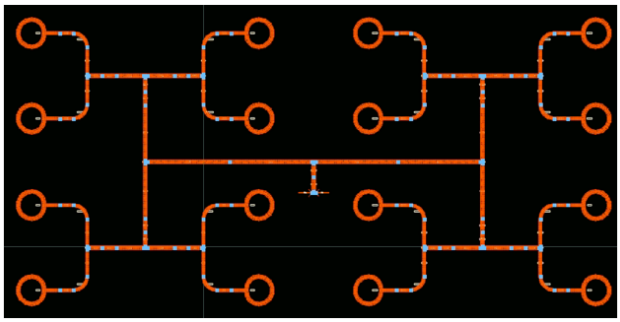

Figure 2. Proposed circular ribbon-shaped antenna array

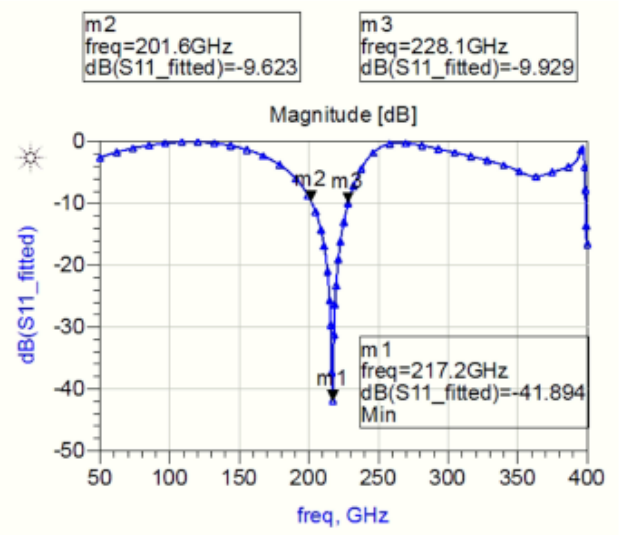

Figure 3. S11 response of proposed antenna design

 DOI: https://doi.org/10.30564/jeisr.v3i1.3550

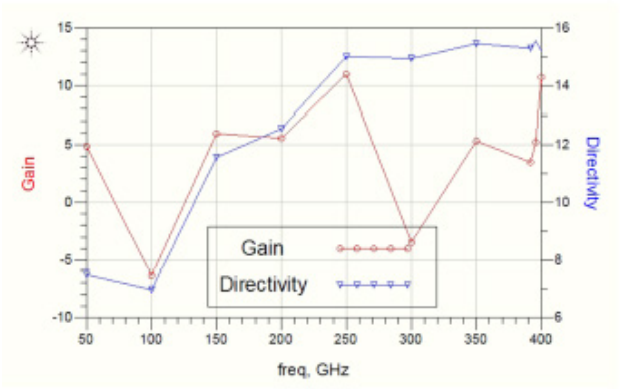

Figure 4. proposed antenna Gain and Directivity

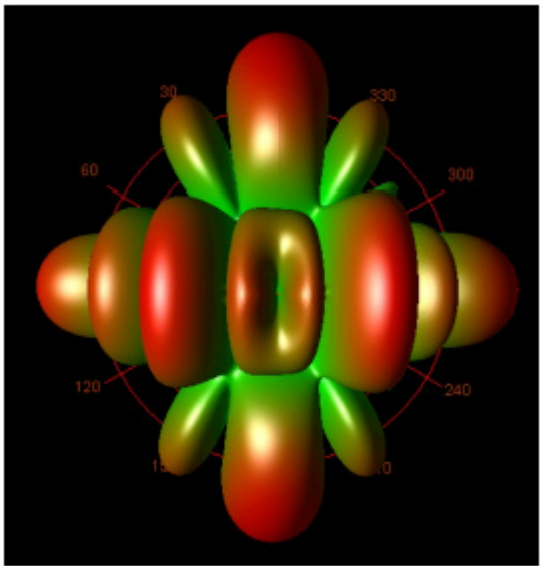

Figure 5. 3D radiation pattern in XY direction

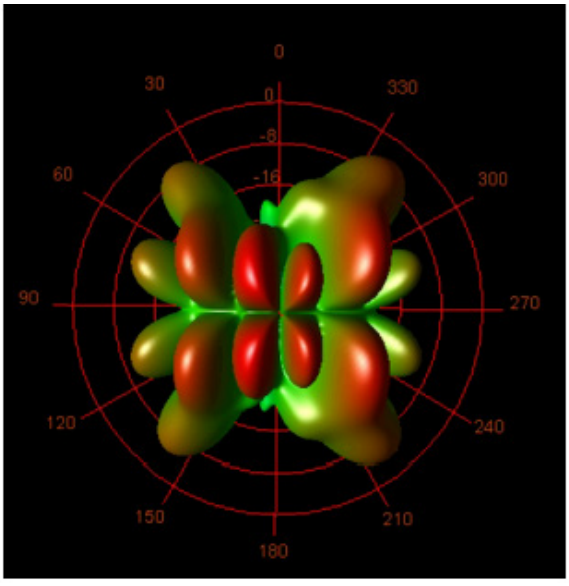

Figure 6. 3D radiation pattern in YZ direction

We would like thank NCTU for providing facilities for our research.

4. Conclusions

In this paper a compact 4 by 4 beamforming antenna array for biomedical application is presented. To enhance the conductivity gold material is used. The proposed antenna operates over the frequency band from 201 GHz to more than 228 GHz. Directivity and gain of the proposed antenna are 13 dB and 7 dB respectively. This makes it applicable for imaging systems because of the frequency band for biomedical imaging.

Acknowledgment

We would like thank NCTU for providing facilities for our research.

References

[1] M. Jenning, B. Klein, R. Hahnel, and D. Plettemeier, "On-Chip Integrated Antennas for 200 GHz Applications," in 2015 IEEE International Conference on Ubiquitous Wireless Broadband (ICUWB), 2015, pp. 1-5.

[2] B. Goettel, P. Pahl, C. Kutschker, S. Malz, U. R. Pfeiffer, and T. Zwick,"Active Multiple Feed On-Chip Antennas With Efficient In-Antenna Power Combining Operating at 200-320 GHz," IEEE Trans. Antennas Propag., vol. 65, no. 2, pp. 416-423, Feb. 2017.

[3] E. H. Frequency, "Supporting innovation in the 100-200 GHz range Proposals to increase access to Extremely High Frequency (EHF) spectrum," no. March, 2020.

[4] S. Gupta, S. Bag, K. Ganguly, I. Sarkar, P. Biswas, and F. I. Conference, Advancements of Medical Electronics. 2015.

[5] S. A. Naghdehforushha and G. Moradi, "Design of plasmonic rectangular ribbon antenna based on graphene for terahertz band communication," IET Microwaves, Antennas Propag., vol. 12, no. 5, pp. 804-807, Apr. 2018.

[6] A. Abohmra, H. Abbas, S. F. Jilani, A. Alomainy, M. A. Imran, and Q. H. Abbasi, "High Bandwidth Perovskite based Antenna for High- Resolution Biomedical Imaging at Terahertz," in 2019 IEEE International Symposium on Antennas and Propagation and USNC-URSI Radio Science Meeting, 2019, pp. 503-504.

[7] Rajinikanth Yella, Krishna Pande, Ke Horng Chen, Edward Chang 28 GHz Monolithic Transmitter on GaN chip for 5G application. The Tenth International

DOI: https://doi.org/10.30564/jeisr.v3i1.3550

Conference on Advances in Satellite and Space Communications SPACOMM 2018.

[8] Rajinikanth Yella, Krishna Pande, Ke Horng Chen, Edward Chang Design of On-Chip GaN transmitter for wireless communication, International Journal On Advances in Telecommunications 2018.

[9] R. HafeziFard, M. Naser-Moghadasi, J. Rashed-Mohassel, and R.-A. Sadeghzadeh Sheikhan, "Mutual Coupling Reduction for Two Closely- Space Meander Line Antennas Using Metamaterial Substrate," IEEE Antennas Wirel. Propag. Lett., vol. 15, pp. 1-1, 2015.

[10] Xin Mi Yang, Xue Guan Liu, Xiao Yang Zhou, and Tie Jun Cui, "Reduction of Mutual Coupling Between Closely Packed Patch Antennas Using Waveguided Metamaterials," IEEE Antennas Wirel. Propag. Lett., vol. 11, pp. 389-391, 2012.

[11] P. Simon, "Analysis and Synthesis of Rotman Lenses," in 22nd AIAA International Communications Satellite Systems Conference Exhibit 2004 (ICSSC), 2004, no. May, pp. 1-11.

[12] S. Vashist, M. K. Soni, and P. K. Singhal, "A Review on the Development of Rotman Lens Antenna," Chinese J. Eng., vol. 2014, no. 11, pp. 1-9, 2014.

 DOI: https://doi.org/10.30564/jeisr.v3i1.3550

Author Guidelines

This document provides some guidelines to authors for submission in order to work towards a seamless submission process. While complete adherence to the following guidelines is not enforced, authors should note that following through with the guidelines will be helpful in expediting the copyediting and proofreading processes, and allow for improved readability during the review process.

Ⅰ. Format

- Program: Microsoft Word (preferred)
- Font: Times New Roman
- Size: 12
- Style: Normal
- Paragraph: Justified
- Required Documents

Ⅱ. Cover Letter

All articles should include a cover letter as a separate document.

The cover letter should include:

- Names and affiliation of author(s)

The corresponding author should be identified.

Eg. Department, University, Province/City/State, Postal Code, Country

- A brief description of the novelty and importance of the findings detailed in the paper

Declaration

v Conflict of Interest

Examples of conflicts of interest include (but are not limited to):

- Research grants
- Honoria
- Employment or consultation
- Project sponsors
- Author’s position on advisory boards or board of directors/management relationships
- Multiple affiliation
- Other financial relationships/support
- Informed Consent

This section confirms that written consent was obtained from all participants prior to the study.

- Ethical Approval

Eg. The paper received the ethical approval of XXX Ethics Committee.

- Trial Registration

Eg. Name of Trial Registry: Trial Registration Number

- Contributorship

The role(s) that each author undertook should be reflected in this section. This section affirms that each credited author has had a significant contribution to the article.

1. Main Manuscript
2. Reference List
3. Supplementary Data/Information

Supplementary figures, small tables, text etc.

As supplementary data/information is not copyedited/proofread, kindly ensure that the section is free from errors, and is presented clearly.

Ⅲ. Abstract

A general introduction to the research topic of the paper should be provided, along with a brief summary of its main results and implications. Kindly ensure the abstract is self-contained and remains readable to a wider audience. The abstract should also be kept to a maximum of 200 words.

Authors should also include 5-8 keywords after the abstract, separated by a semi-colon, avoiding the words already used in the title of the article.

Abstract and keywords should be reflected as font size 14.

Ⅳ. Title

The title should not exceed 50 words. Authors are encouraged to keep their titles succinct and relevant.

Titles should be reflected as font size 26, and in bold type.

Ⅳ. Section Headings

Section headings, sub-headings, and sub-subheadings should be differentiated by font size.

Section Headings: Font size 22, bold type

Sub-Headings: Font size 16, bold type

Sub-Subheadings: Font size 14, bold type

Main Manuscript Outline

Ⅴ. Introduction

The introduction should highlight the significance of the research conducted, in particular, in relation to current state of research in the field. A clear research objective should be conveyed within a single sentence.

Ⅵ. Methodology/Methods

In this section, the methods used to obtain the results in the paper should be clearly elucidated. This allows readers to be able to replicate the study in the future. Authors should ensure that any references made to other research or experiments should be clearly cited.

Ⅶ. Results

In this section, the results of experiments conducted should be detailed. The results should not be discussed at length in

this section. Alternatively, Results and Discussion can also be combined to a single section.

Ⅷ. Discussion

In this section, the results of the experiments conducted can be discussed in detail. Authors should discuss the direct and indirect implications of their findings, and also discuss if the results obtain reflect the current state of research in the field. Applications for the research should be discussed in this section. Suggestions for future research can also be discussed in this section.

Ⅸ. Conclusion

This section offers closure for the paper. An effective conclusion will need to sum up the principal findings of the papers, and its implications for further research.

Ⅹ. References

References should be included as a separate page from the main manuscript. For parts of the manuscript that have referenced a particular source, a superscript (ie. [x]) should be included next to the referenced text.

[x] refers to the allocated number of the source under the Reference List (eg. [1], [2], [3])

In the References section, the corresponding source should be referenced as:

[x] Author(s). Article Title [Publication Type]. Journal Name, Vol. No., Issue No.: Page numbers. (DOI number)

Ⅺ. Glossary of Publication Type

J = Journal/Magazine

M = Monograph/Book

C = (Article) Collection

D = Dissertation/Thesis

P = Patent

S = Standards

N = Newspapers

R = Reports

Kindly note that the order of appearance of the referenced source should follow its order of appearance in the main manuscript.

Graphs, Figures, Tables, and Equations

Graphs, figures and tables should be labelled closely below it and aligned to the center. Each data presentation type should be labelled as Graph, Figure, or Table, and its sequence should be in running order, separate from each other.

Equations should be aligned to the left, and numbered with in running order with its number in parenthesis (aligned right).

Ⅻ. Others

Conflicts of interest, acknowledgements, and publication ethics should also be declared in the final version of the manuscript. Instructions have been provided as its counterpart under Cover Letter.

BILINGUAL PUBLISHING CO.
Pioneer of Global Academics Since 1984

Journal of Electronic & Information Systems

Aims and Scope

Journal of Electronic & Information Systems publishes original research papers that offers professional review and publication to freely disseminate research findings in areas of Networks and Telecommunication, Human–Computer Interaction, Data Management, High Voltage Engineering and more. The Journal focuses on innovations of research methods at all stages and is committed to providing theoretical and practical experience for all those who are involved in these fields.

Journal of Electronic & Information Systems aims to discover innovative methods, theories and studies in its field by publishing original articles, case studies and comprehensive reviews.

The scope of the papers in this journal includes, but is not limited to:

- Networks and Telecommunication
- Human–Computer Interaction
- Data Management
- High Voltage Engineering
- E-Learning Technologies
- E-Commerce Technology
- Computation
- Power Electronics
- Digital Control Systems
- Electronic Ignition Systems
- Digital Communication systems
- Analytics, Business Intelligence and Decision Support Systems

Bilingual Publishing Co. (BPC)

Tel:+65 65881289

E-mail:contact@bilpublishing.com

Website:www.bilpublishing.com

About the Publisher

Bilingual Publishing Co. (BPC) is an international publisher of online, open access and scholarly peer-reviewed journals covering a wide range of academic disciplines including science, technology, medicine, engineering, education and social science. Reflecting the latest research from a broad sweep of subjects, our content is accessible world-wide——both in print and online.

BPC aims to provide an analytics as well as platform for information exchange and discussion that help organizations and professionals in advancing society for the betterment of mankind. BPC hopes to be indexed by well-known databases in order to expand its reach to the science community, and eventually grow to be a reputable publisher recognized by scholars and researchers around the world.

BPC adopts the Open Journal Systems, see on ojs.bilpublishing.com

Database Inclusion

Asia & Pacific Science Citation Index

Creative Commons

China National Knowledge Infrastructure

Google Scholar

Crossref

MyScienceWork

BILINGUAL
PUBLISHING CO.
Pioneer of Global Academics Since 1984

Tel: +65 65881289
E-mail: contact@bilpublishing.com
Website: ojs.bilpublishing.com

ISSN 2661-3204
01